

The Golden Ratio Primal-Dual Algorithm with Two New Step-size Rules for Convex-Concave Saddle Point Problems

Santanu Soe^{a,b}, Matthew K. Tam^b, and V. Vetrivel^a

^aDepartment of Mathematics, Indian Institute of Technology Madras, Chennai 600036, Tamil Nadu, India; ^bSchool of Mathematics and Statistics, The University of Melbourne, Parkville, Melbourne, 3010, Victoria, Australia.

ARTICLE HISTORY

Compiled February 26, 2025

ABSTRACT

In this paper, we present two step-size rules for the extended Golden Ratio primal-dual algorithm (E-GRPDA) designed to address structured convex optimization problems in finite-dimensional real Hilbert spaces. The first rule features a non-increasing primal step-size that remains bounded below by a positive constant and is updated adaptively at each iteration, eliminating the need for the Lipschitz constant of the gradient of the function and the norm of the operator involved. The second step-size rule is adaptive, adjusting based on the local smoothness of the smooth component function and the local estimate of the norm of the operator. In other words, we present an adaptive version of the E-GRPDA algorithm. Importantly, both methods avoid the use of backtracking to estimate the operator norm. We prove that E-GRPDA achieves an ergodic sublinear convergence rate with both step-size rules, evaluated using the primal-dual gap function. Additionally, we establish an R-linear convergence rate for E-GRPDA with the first step-size rule, under some standard assumptions and with appropriately chosen parameters. Through numerical experiments on various convex optimization problems, we demonstrate the effectiveness of our approaches and compare their performance to the existing ones.

KEYWORDS

GRPDA; Primal-dual problems; Partially Adaptive methods; Golden Ratio; Saddle point problems; Adaptive algorithms, Signal recovery

1. Introduction

Let \mathbb{X} and \mathbb{Y} be finite-dimensional real Hilbert spaces. In this paper, we consider the following structured optimization problem

$$\min_{x \in \mathbb{X}} f(x) + g(Kx) + h(x), \quad (1)$$

where $f : \mathbb{X} \rightarrow (-\infty, \infty]$ and $g : \mathbb{Y} \rightarrow (-\infty, \infty]$ are convex, proper, and lower semi-continuous (lsc) functions, $K : \mathbb{X} \rightarrow \mathbb{Y}$ is a linear operator, and $h : \mathbb{X} \rightarrow \mathbb{R}$ is a convex,

CONTACT Santanu Soe. Email: ma22d002@smail.iitm.ac.in, santanu.soe@student.unimelb.edu.au

CONTACT Matthew K. Tam. Email: matthew.tam@unimelb.edu.au

CONTACT V. Vetrivel. Email: vetri@iitm.ac.in

differentiable function with \bar{L} -Lipschitz continuous gradient, i.e.,

$$\|\nabla h(x) - \nabla h(y)\| \leq \bar{L}\|x - y\|, \quad \forall x, y \in \mathbb{X}.$$

The Fenchel dual problem of (1) is given by

$$\max_{u \in \mathbb{Y}} -(f + h)^*(-K^*u) - g^*(u), \quad (2)$$

where $g^*(y) = \sup_{z \in \mathbb{Y}} \{\langle y, z \rangle - g(z)\}$ denotes the *Legendre–Fenchel conjugate* of g and K^* is the adjoint of the linear operator K .

A notable example of a problem in the form of (1) is the *Fused LASSO problem* [35,41], which is commonly used in areas such as genomics, signal processing, and image segmentation. This problem takes the form

$$\min_{x \in \mathbb{R}^n} F(x) := \lambda_1 \|x\|_1 + \lambda_2 \|Dx\|_1 + \frac{1}{2} \|Ax - b\|^2, \quad (3)$$

which corresponds to (1) with $f(x) = \lambda_1 \|x\|_1$, $g(x) = \lambda_2 \|x\|_1$, $K = D$, and $h(x) = \frac{1}{2} \|Ax - b\|^2$, where $A \in \mathbb{R}^{m \times n}$, $b \in \mathbb{R}^m$, and $D \in \mathbb{R}^{(n-1) \times n}$ is the *difference operator* [39]. Here, $\lambda_1, \lambda_2 > 0$ are regularization parameters. Furthermore, when $\lambda_2 = 0$, (3) reduces to the well-known *LASSO problem* [34], which is a particular case of (1) when $h = 0$. Another relevant example of (1) is the *Elastic Net regularization* [45], which combines both ℓ_1 and ℓ_2 penalties. This approach is particularly effective for high-dimensional data where predictors are highly correlated or outnumber the observations, as it balances sparsity and grouping effects to enhance predictive accuracy and interpretability. Given $f(x) = \|x\|_1$, $g(x) = \frac{1}{2} \|x - b\|^2$, and $h(x) = \lambda_2 \|x\|^2$, where $K \in \mathbb{R}^{m \times n}$, $b \in \mathbb{R}^m$, and $\lambda_1, \lambda_2 > 0$ are regularization parameters, the Elastic Net problem can be written as

$$\min_{x \in \mathbb{R}^n} F(x) := \lambda_1 \|x\|_1 + \frac{1}{2} \|Kx - b\|^2 + \lambda_2 \|x\|^2. \quad (4)$$

In addition to these, optimization problems of the form (1) are prevalent in various other fields, such as image denoising, machine learning, game theory, operations research, and many more, see, [4,6,12,16,26,40,44] and references therein.

The convex minimization problem (1) can be solved using the Forward-Backward type splitting methods [1,20,27], provided that the *proximal operator* of $f + g \circ K$ can be computed efficiently. However, in practice, this can be challenging even for simple nonsmooth function g . For instance, consider the case where $g(x) = \|x\|_1$, and $f = 0$. It is well known that the proximal map of g is given by the *soft thresholding operator*, while there is no closed-form solution for the proximal operator of $g \circ K$ when K is not an orthogonal or diagonal matrix, see [28, Section 2.2]. To overcome this difficulty, we can decouple g and K by introducing g^* into (1). This gives the *saddle point* formulation of the problem as

$$\min_{x \in \mathbb{X}} \max_{y \in \mathbb{Y}} \mathcal{L}(x, y) := f(x) + h(x) + \langle Kx, y \rangle - g^*(y). \quad (5)$$

Under strong duality, the saddle point formulation (5) represents a framework for simultaneously solving both the primal problem (1) and the dual problem (2). We begin by reviewing the literature when the smooth term $h = 0$ and then proceed to

discuss the scenario when h is nonzero.

Case 1 ($h = 0$): To solve (1) and (2), a classical primal-dual approach is the *alternating direction methods of multipliers* (ADMM); see, for example, [14,15,20]. Although ADMM can directly be applied to solve $\min_x f(x) + (g \circ K)(x)$, it requires knowledge of the proximal operator of $g \circ K$, which can be challenging, as highlighted in the example mentioned earlier. To utilize the proximal operators of f and g separately, we can introduce a new variable z and reformulate $\min_x f(x) + g(Kx)$ as

$$\min_{x,z} f(x) + g(z) \text{ subject to } Kx - z = 0. \quad (6)$$

Now, applying ADMM to (6) results in the following iterative updates

$$\begin{cases} x_{n+1} = \arg \min_x f(x) + \frac{\delta'}{2} \|Kx - z_n + u_n\|^2, \\ z_{n+1} = \arg \min_z g(z) + \frac{\delta'}{2} \|Kx_{n+1} - z + u_n\|^2, \\ u_{n+1} = u_n + Kx_{n+1} - z_{n+1}, \end{cases} \quad (7)$$

where $\delta' > 0$. Although the z -update of (7) can be computed easily if the proximal operator of g is known, solving the x -update requires an iterative approach and the assumption that K has a full rank. Under the assumption $\text{rank } K = \dim \mathbb{Y}$, the x -update can be written as $x_{n+1} = \text{prox}_{\frac{K^*K}{\delta'} f}((K^*K)^{-1}K^*(z_n - u_n))$, where $\text{prox}_{\frac{K^*K}{\delta'} f}$ is the generalized proximal operator [29,42], which restricts the possible choices for K . Moreover, when $g(x) = \frac{1}{2}\|x - b\|^2$ and $f = 0$, solving the z -update in (7) is equivalent to solving the linear system

$$(K^*K + \delta'I)z_{n+1} = K^*b + \delta'u_n + \delta'Kx_{n+1}.$$

For large, dense matrices, efficiently solving such systems becomes challenging due to the substantial memory required to store the matrix during computation. These limitations can be circumvented by employing a simple primal-dual approach known as the *Arrow–Hurwicz method* [36]. This method leverages the proximal operators of f and g^* individually, which removes the need to solve subproblems or handle systems involving the operator K . Given $(x_0, y_0) \in \mathbb{X} \times \mathbb{Y}$, the iteration scheme for $n \geq 1$ is

$$\begin{cases} x_n = \text{prox}_{\tau f}(x_{n-1} - \tau K^*y_{n-1}), \\ y_n = \text{prox}_{\sigma g^*}(y_{n-1} - \sigma Kx_n), \end{cases} \quad (8)$$

where $\tau, \sigma > 0$ are the primal and dual stepsize parameters, respectively. The convergence of the Arrow–Hurwicz method [36] heavily depends on the choice of objective functions, their domains, and the appropriate selection of stepsizes τ and σ . For example, when the domain of g^* is bounded, the convergence of the method has been established with a convergence rate of $\mathcal{O}(1/\sqrt{N})$, where N is the number of iterations, measured by the primal-dual gap function; see [6,26]. However, the sequence generated by this method does not converge in general; see [17,18] for a series of counterexamples in both one and higher dimensions. To achieve convergence of (8) in more general cases, Chambolle and Pock [6] introduced an extrapolation step in (8) following the computation of the primal variable x_n . For $(x_0, y_0) \in \mathbb{X} \times \mathbb{Y}$, $\delta \in [0, 1]$, and $n \geq 1$, the

Chambolle–Pock primal-dual algorithm iterates as

$$\begin{cases} x_n = \text{prox}_{\tau f}(x_{n-1} - \tau K^* y_{n-1}), \\ \tilde{x}_n = x_n + \delta(x_n - x_{n-1}), \\ y_n = \text{prox}_{\sigma g^*}(y_{n-1} - \sigma K \tilde{x}_n). \end{cases} \quad (9)$$

For $\delta = 0$, the primal-dual algorithm (9) reduces to the Arrow-Hurwicz algorithm (8). Chambolle and Pock proved the convergence of (9) for $\delta = 1$, commonly known as the *Primal-Dual Hybrid Gradient (PDHG)* method. They demonstrated that this method achieves a convergence rate of $\mathcal{O}(1/N)$, measured by the primal-dual gap function, provided that the stepsize condition $\tau\sigma\|K\|^2 < 1$ is satisfied, see, [6, Theorem 1]. Additionally, convergence is also guaranteed when $\tau\sigma\|K\|^2 = 1$, see, [13, Theorem 3.3], which simplifies stepsize selection by reducing it to the tuning of a single parameter. More recently, Chang and Yang introduced a modified version of the Arrow-Hurwicz algorithm called the *Golden Ratio primal-dual algorithm (GRPDA)* [8, Algorithm 3.1]. This algorithm allows for larger primal-dual stepsizes compared to PDHG, with its benefits demonstrated through experimental results [8]. For $(x_0, y_0) \in \mathbb{X} \times \mathbb{Y}$, with $z_0 = x_0$ and $n \geq 1$, the GRPDA iteration scheme is given by

$$\begin{cases} z_n = \frac{\psi - 1}{\psi} x_n + \frac{1}{\psi} z_{n-1}, \\ x_n = \text{prox}_{\tau f}(z_n - \tau K^* y_{n-1}), \\ y_n = \text{prox}_{\sigma g^*}(y_{n-1} - \sigma K x_n). \end{cases} \quad (10)$$

The main difference between the Chambolle-Pock primal-dual algorithm (9) and GRPDA (10) is that, instead of the extrapolation term, a convex combination based on the Golden Ratio is added in the x -subproblem of (8). This convex combination allows GRPDA to converge when the stepsize condition $\tau\sigma\|K\|^2 < \phi$ is satisfied, where ϕ is the Golden Ratio. The authors also demonstrated that GRPDA achieves a convergence rate of $\mathcal{O}(1/N)$, measured by the primal-dual gap function, see [8, Theorem 3.2]. Furthermore, it was shown that a form of (9) with $\delta = 1$ and (10) are equivalent when GRPDA is interpreted as a preconditioned ADMM, see, [8, Section 3] for detailed calculations. When the primal-dual algorithm (9) is interpreted as preconditioned ADMM, the preconditioned matrix must necessarily be positive definite to prove global convergence, which is guaranteed by the stepsize condition $\tau\sigma\|K\|^2 < 1$. However, in the case of GRPDA, the preconditioned matrix is allowed to be indefinite, offering a broader choice of parameters for practical applications. Nevertheless, all the above-mentioned algorithms require the knowledge of the norm of the operator K during the application, which is a disadvantage when the norm is unknown.

Case 2 ($h \neq 0$): When the smooth term is nonzero i.e., ($h \neq 0$), all the aforementioned methods can still be applied by replacing f with $f + h$. However, in this case, computing the proximal operator of $f + h$ could be more challenging than that of f alone. To address this shortcoming, the authors [13,38] extended the PDHG algorithm by incorporating the first-order approximation of the gradient of the differentiable function h into the primal variable updates during the iterations of (9), resulting in the *Condat–Vũ algorithm*. Starting from an initial point $(x_0, y_0) \in \mathbb{X} \times \mathbb{Y}$

and for $n \geq 1$, the steps of the Condat–Vũ algorithm proceed as follows

$$\begin{cases} x_n = \text{prox}_{\tau f}(x_{n-1} - \tau K^* y_{n-1} - \tau \nabla h(x_{n-1})), \\ \tilde{x}_n = x_n + \delta(x_n - x_{n-1}), \\ y_n = \text{prox}_{\sigma g^*}(y_{n-1} - \sigma K \tilde{x}_n). \end{cases} \quad (11)$$

In this case, the sequences generated by (11) converge under the stepsize condition $\tau\sigma\|K\|^2 + \tau\bar{L}/2 \leq 1$. In recent years, various three-operator primal-dual algorithms, akin to the Condat–Vũ algorithm, have been developed to address the problem (1). These algorithms ensure global convergence by requiring a stepsize inequality that depends on both the $\|K\|$ and the Lipschitz constant \bar{L} . Notable examples include the *primal-dual fixed point algorithm* (PDFP) [11], the *primal-dual three-operator splitting* (PD3O) [39], and the *primal-dual Davis–Yin splitting* (PDDY) [31], all of which share the stepsize condition $\tau\sigma\|K\|^2 < 1$ and $\tau\bar{L} < 2$, ensuring convergence to a saddle point under the assumptions of convexity and global Lipschitz continuity of the gradient of the smooth function. More recently, Malitsky and Tam [25] developed a three-operator primal-dual algorithm, also known as the *primal-dual twice reflected* (PDTR) method, which converges globally under the stepsize condition $\tau\sigma\|K\|^2 + 2\tau\bar{L} < 1$. Since GRPDA (10) can be seen as an extension of the PDHG algorithm for $h = 0$, Zhou et al. [43] similarly extended GRPDA (10) to the three-operator splitting (i.e., $h \neq 0$) settings, referred to as the *extended Golden Ratio primal-dual algorithm* (E-GRPDA). Given $(x_0, y_0) \in \mathbb{X} \times \mathbb{Y}$ with $z_0 = x_0$, E-GRPDA iterates as

$$\begin{cases} z_n = \frac{\psi - 1}{\psi} x_n + \frac{1}{\psi} z_{n-1}, \\ x_n = \text{prox}_{\tau f}(z_n - \tau K^* y_{n-1} - \tau \nabla h(x_{n-1})), \\ y_n = \text{prox}_{\sigma g^*}(y_{n-1} + \sigma K x_n). \end{cases} \quad (12)$$

The sequence generated by (12) converges, as measured by the function value residual and constraint violation, provided the stepsize condition $\tau\sigma\|K\|^2 + 2\tau\bar{L}(1 - \mu) \leq \psi(1 - \mu)$ is satisfied with $\mu \in (0, 1)$ and $\psi \in (1, \phi]$.

Nonetheless, in all the aforementioned primal-dual algorithms and their extensions, prior knowledge of the operator norm of K and the Lipschitz constants \bar{L} is required to select appropriate values for τ and σ to achieve the desired numerical performance within a given number of iterations. These requirements are often impractical or expensive to compute for many optimization problems. For example, in CT image reconstruction [32], the exact spectral norm of K is typically large, dense, and expensive to compute. Therefore, for scenarios like this, we need stepsizes that do not depend on the parameters \bar{L} and $\|K\|$. To avoid this setback, Malitsky and Pock [24] incorporate a backtracking linesearch strategy into a version of the Condat–Vũ algorithm (11). However, it still requires global Lipschitzness of ∇h . In a similar manner, Chang et al. [10] also introduced the linesearch technique into (10) to remove the dependency on $\|K\|$. While linesearch enables the algorithm to adaptively determine appropriate stepsizes during execution, it requires an inner loop within each outer iteration to run until a stopping criterion is met, which can be time-consuming.

To mitigate the limitations of linesearch, adaptive methods offer effective alternatives by refining poor initial stepsizes and eliminating dependence on global Lipschitz continuity by exploiting the approximation of the inverse local Lipschitz constant. In light of this idea, several authors have developed adaptive methods for different

cases of (1). In 2019, Malitsky and Michenko [22] proposed an adaptive stepsize rule for (1) when $f = g = 0$, using the local information of the gradient of h . More recently, Vladarean et al. [37] introduced an *adaptive primal-dual algorithm* (APDA) for a special case of (1) when $f = 0$, which also uses the local information of ∇h around the current iterates but still requires the knowledge of $\|K\|$. Building on similar concepts, Latafat et al. [19] introduced a *fully adaptive three-operator splitting method* (adaPDM+) to solve (1) by leveraging the local Lipschitz continuity of ∇h and incorporating a linesearch technique to remove the reliance on $\|K\|$ as a parameter. Independently, Malitsky and Mishchenko [23] extended their works from [22] and proposed the *adaptive proximal gradient method* (AdaProxGD) for the special case of (1) when $g = 0$. Given the limitations of linesearch, we aim to develop an adaptive algorithm for (1) that utilizes both the local estimates of the Lipschitz constant \bar{L} and the operator norm of K .

In 2020, Malitsky [21, Algorithm 1] proposed an *adaptive Golden Ratio algorithm* (aGRAAL) for solving mixed variational inequality problems (MVIP) that adapts to local smoothness similarly to the methods in [32,37]. This method addresses the following MVIP for a given monotone, locally Lipschitz continuous function F on a finite-dimensional Hilbert space \mathcal{V}

$$\text{Find } u^* \in \mathcal{V} \text{ such that } \langle F(u^*), u - u^* \rangle + \theta(u) - \theta(u^*) \geq 0, \forall u \in \mathcal{V}. \quad (13)$$

The framework of (13) can be recovered by writing the optimality conditions of (1) and taking $u = (x, y)$ with $F(u) = (\nabla h(x) + K^*y, -Kx)$ and $\theta(u) = f(x) + g^*(y)$. However, as pointed out in [8,37], if aGRAAL is applied to this derived variational inequality framework of (1) with $u = (x, y), v = (z, w) \in \mathcal{V} = \mathbb{X} \times \mathbb{Y}$, and the inner product $\langle (x, y), (z, w) \rangle = \langle x, z \rangle + \langle y, w \rangle$, the following primal-dual algorithm is obtained

Algorithm 1 aGRAAL

1: **Step 0:** Let $x_0, x_1 \in \mathbb{X}, y_0, y_1 \in \mathbb{Y}, (\bar{x}_0, \bar{y}_0) = (x_0, y_0)$. Set $\lambda_0 > 0, \psi \in (1, \phi]$, where ϕ is the Golden Ratio, $\rho = \frac{1}{\psi} + \frac{1}{\psi^2}, \theta_0 > 0$, and $\bar{\lambda} \gg 0$.

2: **Step 1:** *Update*

$$\lambda_n = \min \left\{ \rho \lambda_{n-1}, \frac{\psi \theta_{n-1}}{4 \lambda_{n-1}} \frac{\|u_n - u_{n-1}\|^2}{\|F(u_n) - F(u_{n-1})\|^2}, \bar{\lambda} \right\}.$$

3: **Step 2:** *Compute*

$$\begin{aligned} \bar{x}_n &= \frac{(\psi - 1)x_n + \bar{x}_{n-1}}{\psi}, & x_{n+1} &= \text{prox}_{\lambda_n f}(\bar{x}_n - \lambda_n K^* y_n - \lambda_n \nabla h(x_n)), \\ \bar{y}_n &= \frac{(\psi - 1)y_n + \bar{y}_{n-1}}{\psi}, & y_{n+1} &= \text{prox}_{\lambda_n g^*}(\bar{y}_n + \lambda_n K x_n). \end{aligned} \quad (14)$$

4: **Step 3:** *Update*

$$\theta_n = \psi \frac{\lambda_n}{\lambda_{n-1}}.$$

5: **Step 4:** Let $n \leftarrow n + 1$ and return to Step 1.

The Algorithm 1 presented above is a Jacobian-type algorithm that does not lever-

age information from the current iterate. More precisely, the immediate primal update x_{n+1} is not used in calculating the subsequent dual update y_{n+1} . Furthermore, in both the x - and y - subproblems of (14), the primal and dual stepsizes are equal, which can be limiting as it may result in poorer convergence bounds. Therefore, a fully adaptive method that performs updates in a Gauss–Seidel fashion at each iteration would be beneficial, allowing for efficient resolution of (12) while leveraging the problem’s inherent structure.

1.1. Motivations and Contributions

Our main motivation is to propose new stepsize rules for the extended Golden Ratio primal-dual algorithm (12), where the primal-dual stepsizes are independent of the parameters $\|K\|$ and \bar{L} . Broadly speaking, our motivations are twofold: Firstly, we propose a new stepsize rule for E-GRPDA (12), where the primal stepsize τ_n is non-increasing and separated from zero. The existence of the global Lipschitz constant \bar{L} is sufficient to prove the global convergence of our proposed Algorithm 2. However, verifying the global smoothness property can be challenging, particularly when h is a complex nonsmooth function. Additionally, Algorithm 2 may experience slower convergence and require more iterations to reach a specified error bound, as the stepsize τ_n is nonincreasing. Secondly, to mitigate the above difficulties, we propose an adaptive method (Algorithm 3) for (12), where the primal stepsize τ_n adapts to the local geometry around the norm of the operator and the gradient of h , thereby eliminating the dependency on $\|K\|$ as well as global smoothness of h . In Algorithm 3, the stepsize τ_n is allowed to adaptively increase and decrease while preserving all the favorable convergence properties.

The rest of this paper outlines the following contributions:

- In Section 2, we discuss some useful lemmas and blanket assumptions that apply to the proposed algorithms throughout the paper. We also define the primal-dual gap function needed for convergence analysis.
- In Section 3, we analyze the extended GRPDA (12) with a new stepsize rule proposed in Algorithm 2, which, unlike traditional approaches, does not require knowledge of \bar{L} and eliminates the need for backtracking by using the estimates of $\|K\|$ around the current iterates. We establish both global iterate convergence and an ergodic $\mathcal{O}(1/N)$ rate of convergence, where N is the iteration count, as measured by the primal-dual gap function. By carrying out refined analysis, we extend the region of convergence of Algorithm 2 from $(1, \phi]$ to $(1, 1 + \sqrt{3})$ as it was done for GRPDA (10) in [9]. Furthermore, we show that when the initial primal stepsize τ_0 is less than or equal to the positive constant $\min\{\frac{\mu}{\sqrt{\beta}\|K\|}, \frac{\mu'}{\bar{L}}\}$, the stepsize condition for (12) can still be recovered, which is an advancement for the E-GRPDA algorithm.
- In Section 4, we demonstrate nonergodic R-linear convergence rate of Algorithm 2 when both g^* and h are strongly convex functions under some appropriate parameter choices.
- In Section 5, we introduce an adaptive stepsize rule to solve (12) as formulated in Algorithm 3, where the stepsize τ_n can increase in flatter regions, unlike in Algorithm 2. This method, like Algorithm 2, does not require backtracking to eliminate the need for knowledge of the norm of K and further improves upon Algorithm 2 by using the local Lipschitz information of ∇h instead of relying

on global Lipschitz continuity. Moreover, it can readily adjust to poor initial stepsizes by adapting to the local geometry of the smooth function h . We establish the global convergence of the method and demonstrate an $\mathcal{O}(1/N)$ rate of convergence, similar to other adaptive primal-dual methods such as APDA and adaPDM+, etc.

- Section 6 presents numerical experiments on various problems, including LASSO, Non-negative least squares, Fused LASSO, and Elastic Net regularization. We demonstrate the applicability and performance of the proposed strategies, showing that they outperform existing methods.

2. Preliminaries and Assumptions

Throughout this paper, we denote the Golden Ratio by $\phi = \frac{1+\sqrt{5}}{2}$. The norm of a linear operator $K : \mathbb{X} \rightarrow \mathbb{Y}$ is defined by $\|K\| = \sup\{\|Kx\| : \|x\| = 1, x \in \mathbb{X}\}$.

Given a proper, convex and lsc function $f : \mathbb{X} \rightarrow (-\infty, \infty]$, the *effective domain* of f is given by $\text{dom}(f) = \{x \in \mathbb{X} : f(x) < +\infty\}$. The *subdifferential* of f at $x^* \in \text{dom}(f)$ is denoted by $\partial f(x^*)$, and $\partial f : \mathbb{X} \rightarrow 2^{\mathbb{X}}$ is defined as

$$\partial f(x^*) = \{v \in \mathbb{X} : f(x) \geq f(x^*) + \langle v, x - x^* \rangle \ \forall x \in \mathbb{X}\}.$$

For $\beta > 0$, the *proximal operator* [30, Example 2.5.1] of f with the parameter β is given by

$$\text{prox}_{\beta f}(x) = \arg \min_{y \in \mathbb{X}} \left\{ f(y) + \frac{1}{2\beta} \|y - x\|^2 \right\}.$$

For any $\beta > 0$, the proximal operator $\text{prox}_{\beta h}$ is well defined, see [30, Section 1.3.11]. Now, we are ready to state the following lemma.

Lemma 2.1. [2, Proposition 12.26] *Suppose that $f : \mathbb{X} \rightarrow (-\infty, \infty]$ is a proper, convex and lsc function. Then, for any $x \in \mathbb{X}$ and $\lambda > 0$, we have $\tilde{q} = \text{prox}_{\lambda f}(x)$ if and only if*

$$\lambda(f(\tilde{q}) - f(y)) \leq \langle \tilde{q} - x, y - \tilde{q} \rangle, \ \forall y \in \mathbb{X}.$$

Given a non empty set D , the *indicator function* i_D is defined as $i_D(x) = 0$ if $x \in D$, and $i_D(x) = \infty$ otherwise.

Next, we make the following blanket assumptions.

Assumption 2.2. *We assume that the set of solutions of (5) is non-empty. Moreover, it holds that $0 \in \text{ri}(K(\text{dom}(f) - \text{dom}(g)))$*

Here, “ri” denotes the *relative interior* [2, Definition 6.9] of a convex set. Under Assumption 2.2, it follows from [13, Section 2] and [2, Definition 19.16] that a pair (\bar{x}, \bar{y}) is a solution of (5) if and only if \bar{x} and \bar{y} is a solution to the primal problem (1) and the dual problem (2), respectively, which is equivalently characterized by the following inequality

$$\mathcal{L}(\bar{x}, y) \leq \mathcal{L}(\bar{x}, \bar{y}) \leq \mathcal{L}(x, \bar{y}), \ \forall (x, y) \in \mathbb{X} \times \mathbb{Y}. \quad (15)$$

Throughout the paper, we denote Ω as the set of all saddle points of \mathcal{L} , which is nonempty under Assumption 2.2, and is given by

$$\Omega = \{(\bar{x}, \bar{y}) \in \mathbb{X} \times \mathbb{Y} : -K^*\bar{y} \in \partial f(\bar{x}) + \nabla h(\bar{x}), 0 \in \partial g^*(\bar{y}) - K\bar{x}\}. \quad (16)$$

Let $(\bar{x}, \bar{y}) \in \Omega$. Then, for any $(x, y) \in \mathbb{X} \times \mathbb{Y}$, the primal-dual gap function \mathcal{G} is defined as

$$\mathcal{G}(x, y) = \mathcal{L}(x, \bar{y}) - \mathcal{L}(\bar{x}, y). \quad (17)$$

Note that $\mathcal{G}(x, y)$ depends on (\bar{x}, \bar{y}) , which does not need to be mentioned explicitly as it is clear from the context. Moreover, we can rewrite (17) as $\mathcal{G}(x, y) = \mathcal{P}(x) + \mathcal{D}(y)$, where $\mathcal{P}(x)$ and $\mathcal{D}(y)$ are given by

$$\begin{aligned} \mathcal{P}(x) &= \mathcal{L}(x, \bar{y}) - \mathcal{L}(\bar{x}, \bar{y}) = (f + h)(x) - (f + h)(\bar{x}) + \langle K(x - \bar{x}), y - \bar{y} \rangle, \\ \mathcal{D}(y) &= \mathcal{L}(\bar{x}, \bar{y}) - \mathcal{L}(\bar{x}, y) = g^*(y) - g^*(\bar{y}) - \langle K\bar{x}, y - \bar{y} \rangle. \end{aligned} \quad (18)$$

From (15), (17) and (18), it follows that $\mathcal{P}(x)$, $\mathcal{D}(y)$, and $\mathcal{G}(x, y)$ are all convex functions in their respective variables. Additionally, we have $\mathcal{P}(x) \geq 0$, $\mathcal{D}(y) \geq 0$, and $\mathcal{G}(x, y) \geq 0 \forall x, y$. The primal-dual gap function has been used in the analysis of GRPDA and other primal-dual algorithms; for instance, see, [6–8,10,24,37].

Assumption 2.3. *The proximal operators of f and g are “proximal friendly”; that is, the proximal operators of f and g can be evaluated efficiently.*

Both Assumption 2.2 and Assumption 2.3 are common in literature, see [8,10,37]. Note that, under Assumption 2.3, the proximal operator of the conjugate g^* can be computed using the *Moreau decomposition* [3, Theorem 6.45].

We end this section with the following useful lemmas.

Lemma 2.4. [2] *For any $a, b, c \in \mathbb{X}$ and $\alpha \in \mathbb{R}$, we have*

$$\langle a - b, a - c \rangle = \frac{1}{2}\|a - b\|^2 + \frac{1}{2}\|a - c\|^2 - \frac{1}{2}\|b - c\|^2, \quad (19a)$$

$$\|\alpha a + (1 - \alpha)b\|^2 = \alpha\|a\|^2 + (1 - \alpha)\|b\|^2 - \alpha(1 - \alpha)\|a - b\|^2. \quad (19b)$$

Lemma 2.5. [9] *Suppose that (p_n) and (q_n) are two nonnegative real sequences and that there exists a natural number n_0 such that $p_{n+1} \leq p_n - q_n$, $\forall n \geq n_0$. Then, $\sum_{n=1}^{\infty} q_n < \infty$ and $\lim_{n \rightarrow \infty} p_n$ exists.*

Lemma 2.6. *For $m_1, m_2 \in \mathbb{R}$, $p \geq 0$, and $q > 0$, we have $\frac{pq}{p+q}(m_1 + m_2)^2 \leq pm_1^2 + qm_2^2$.*

3. GRPDA with partially adaptive stepsize

In this section, we introduce a partially adaptive stepsize rule for E-GRPDA (12) that neither requires prior knowledge of the norm of the operator K nor the Lipschitz constant \bar{L} as inputs of the algorithm. We refer to this algorithm, which is presented in Algorithm 2, as the partially adaptive Golden Ratio primal-dual algorithm (P-GRPDA). By “partially adaptive,” we indicate that the stepsize τ_n is constrained from increasing at any iteration.

Assumption 3.1. Suppose that f and g are proper, convex and lsc, and h is convex and \bar{L} -smooth.

Algorithm 2 Partially Adaptive GRPDA (P-GRPDA) for (12)

1: **Step 0:** Let $x_0 \in \mathbb{X}$, $y_0 \in \mathbb{Y}$, $z_0 = x_0$, $\beta > 0$, $0 < 2\mu' < \mu < \psi/2$, $\psi \in (1, \phi]$.

Suppose $\tau_0 > 0$ and $n = 1$.

2: **Step 1:** Compute

$$z_n = \frac{\psi - 1}{\psi} x_{n-1} + \frac{1}{\psi} z_{n-1}, \quad (20)$$

$$x_n = \text{prox}_{\tau_{n-1}f}(z_n - \tau_{n-1}K^*y_{n-1} - \tau_{n-1}\nabla h(x_{n-1})). \quad (21)$$

3: **Step 2:** Update

$$\tau_n = \min \left\{ \tau_{n-1}, \frac{\mu \|x_n - x_{n-1}\|}{\sqrt{\beta} \|Kx_n - Kx_{n-1}\|}, \frac{\mu' \|x_n - x_{n-1}\|}{\|\nabla h(x_n) - \nabla h(x_{n-1})\|} \right\}, \quad (22)$$

$$\sigma_n = \beta \tau_n.$$

4: **Step 3:** Compute

$$y_n = \text{prox}_{\sigma_n g^*}(y_{n-1} + \sigma_n Kx_n). \quad (23)$$

5: **Step 4:** Let $n \leftarrow n + 1$ and return to Step 1.

Before turning our attention to the convergence analysis, some comments regarding Algorithm 2 are in order.

Remark 3.2. Here, $\beta > 0$ is an algorithmic parameter to maintain the balance in convergence by scaling the dual steps. In (22), when $Kx_n = Kx_{n-1}$ or $\nabla h(x_n) = \nabla h(x_{n-1})$ holds for some n , we adopt the convention that $1/0 = \infty$. Under this convention, the stepsize τ_n is chosen as the minimum of τ_{n-1} and the value of the last two terms in (22) whose denominator is nonzero. Additionally, if $x_n = x_{n-1}$, we adopt the convention $\frac{0}{0} = \infty$, and set $\tau_n = \tau_{n-1}$. Moreover, when $Kx_n = Kx_{n-1}$ and $\nabla h(x_n) = \nabla h(x_{n-1})$ simultaneously hold for some n , the convention $\frac{1}{0} = \infty$ ensures that τ_n defaults to the previous primal stepsize τ_{n-1} .

Remark 3.3. From (22), it follows that (τ_n) is nonincreasing, which may slow down Algorithm 2 for a given convergence bound. However, larger μ and μ' for a given ψ play a crucial role in estimating $\|K\|$ and \bar{L} . Therefore, in practice, the largest pair (μ, μ') is selected for a given ψ . In Theorem 3.8, we extend the allowable values of μ and μ' for $1 < \psi < 1 + \sqrt{3}$, and the selection of the largest pairs for a given ψ is illustrated in Figure 1.

Next, we present the following proposition.

Proposition 3.4. Let (τ_n) be the stepsize sequence generated by Algorithm 2. Then, (τ_n) is bounded below by $\eta = \min \left\{ \tau_0, \frac{\mu}{\sqrt{\beta}\|K\|}, \frac{\mu'}{\bar{L}} \right\}$ and $\lim_{n \rightarrow \infty} \tau_n \geq \eta > 0$.

Proof. We use induction to prove our first claim. First note that, from the definition of

τ_n in (22), we have $\tau_n \leq \tau_{n-1}$, $\forall n \geq 1$. Noting the conventions described in Remark 3.2, the definition of $\|K\|$ together with Lipschitz continuity of ∇h yields the following inequality for all $n \geq 1$

$$\begin{aligned} \tau_n &= \min \left\{ \tau_{n-1}, \frac{\mu \|x_n - x_{n-1}\|}{\sqrt{\beta} \|Kx_n - Kx_{n-1}\|}, \frac{\mu' \|x_n - x_{n-1}\|}{\|\nabla h(x_n) - \nabla h(x_{n-1})\|} \right\} \\ &\geq \min \left\{ \tau_{n-1}, \frac{\mu}{\sqrt{\beta} \|K\|}, \frac{\mu'}{\bar{L}} \right\}. \end{aligned} \quad (24)$$

Now, for $n = 1$, from (24), we have $\tau_1 \geq \eta$, where $\eta = \min \left\{ \tau_0, \frac{\mu}{\sqrt{\beta} \|K\|}, \frac{\mu'}{\bar{L}} \right\}$. Suppose $\tau_n \geq \eta$ holds for some n . Then, by induction and (24), we have

$$\tau_{n+1} \geq \min \left\{ \tau_n, \frac{\mu}{\sqrt{\beta} \|K\|}, \frac{\mu'}{\bar{L}} \right\} \geq \eta. \quad (25)$$

Therefore, we conclude the first claim of our proof. For the second claim, note that the sequence (τ_n) is nonincreasing and bounded below by $\eta > 0$. Consequently, this implies that (τ_n) is convergent and $\lim_{n \rightarrow \infty} \tau_n = \tau \geq \eta > 0$ for some $\tau > 0$. \square

3.1. Convergence analysis

In this section, we establish the convergence of Algorithm 2.

Lemma 3.5. *Let $(\bar{x}, \bar{y}) \in \mathcal{S}$. Under Assumptions 2.2, 2.3 and 3.1, let $\{(z_n, x_n, \tau_n, y_n)\}$ be the sequence generated by Algorithm 2. Then, there exists a natural number n_2 such that, $\forall n \geq n_2$, the following holds*

$$\begin{aligned} &2\tau_n \mathcal{G}(x_n, y_n) + \frac{\psi}{\psi - 1} \|\bar{x} - z_{n+2}\|^2 + \frac{1}{\beta} \|y - y_n\|^2 + \mu' \|x_n - x_{n+1}\|^2 \\ &\leq \frac{\psi}{\psi - 1} \|\bar{x} - z_{n+1}\|^2 + \frac{1}{\beta} \|\bar{y} - y_{n-1}\|^2 + \mu' \|x_n - x_{n-1}\|^2 - \psi \bar{\theta}_n \|x_n - z_{n+1}\|^2, \end{aligned} \quad (26)$$

where $\bar{\theta}_n = \frac{\tau_n}{\tau_{n-1}}$.

Proof. Using (21), (23), Lemma 2.1, and the fact $\sigma_n = \beta \tau_n$ from (22), we obtain the following inequalities

$$\begin{aligned} \tau_n (f(x_{n+1}) - f(\bar{x})) &\leq \langle x_{n+1} - z_{n+1} + \tau_n K^* y_n + \tau_n \nabla h(x_n), \bar{x} - x_{n+1} \rangle, \\ \tau_n (g^*(y_n) - g^*(\bar{y})) &\leq \left\langle \frac{1}{\beta} (y_n - y_{n-1}) - \tau_n K x_n, \bar{y} - y_n \right\rangle. \end{aligned} \quad (27)$$

Similarly, using the fact that $x_n - z_n = \psi(x_n - z_{n+1})$, we get

$$\begin{aligned} \tau_{n-1} (f(x_n) - f(x_{n+1})) &\leq \langle x_n - z_n + \tau_{n-1} K^* y_{n-1} + \tau_{n-1} \nabla h(x_{n-1}), x_{n+1} - x_n \rangle \\ &= \langle \psi(x_n - z_{n+1}) + \tau_{n-1} K^* y_{n-1} + \tau_{n-1} \nabla h(x_{n-1}), x_{n+1} - x_n \rangle. \end{aligned} \quad (28)$$

Multiplying (28) by $\bar{\theta}_n = \frac{\tau_n}{\tau_{n-1}}$ followed by adding two inequalities in (27) gives

$$\begin{aligned} \tau_n(f(x_n) - f(\bar{x}) + g^*(y_n) - g^*(\bar{y})) &\leq \langle x_{n+1} - z_{n+1}, \bar{x} - x_{n+1} \rangle \\ &+ \langle \psi \bar{\theta}_n(x_n - z_{n+1}), x_{n+1} - x_n \rangle + \frac{1}{\beta} \langle y_n - y_{n-1}, \bar{y} - y_n \rangle + \tau_n \langle K^* y_{n-1}, x_{n+1} - x_n \rangle \\ &+ \tau_n \langle K^* y_n, \bar{x} - x_{n+1} \rangle - \tau_n \langle K x_n, \bar{y} - y_n \rangle + \tau_n \langle \nabla h(x_{n-1}), x_{n+1} - x_n \rangle \\ &+ \tau_n \langle \nabla h(x_n), \bar{x} - x_{n+1} \rangle. \end{aligned} \quad (29)$$

By adding $\tau_n(h(x_n) - h(\bar{x}))$ to both sides of (29) and performing some straightforward calculations, we obtain

$$\begin{aligned} \tau_n(\mathcal{L}(x_n, \bar{y}) - \mathcal{L}(\bar{x}, y_n)) &\leq \langle x_{n+1} - z_{n+1}, \bar{x} - x_{n+1} \rangle \\ &+ \psi \langle \bar{\theta}_n(x_n - z_{n+1}), x_{n+1} - x_n \rangle + \frac{1}{\beta} \langle y_n - y_{n-1}, y - y_n \rangle \\ &+ \langle K(x_n - x_{n+1}), y_n - y_{n-1} \rangle + \tau_n \langle \nabla h(x_{n-1}), x_{n+1} - x_n \rangle \\ &+ \tau_n(h(x_n) - h(\bar{x}) + \langle \nabla h(x_n), \bar{x} - x_{n+1} \rangle). \end{aligned} \quad (30)$$

Now, by using the convexity of h and the definition of \mathcal{G} , we obtain

$$\begin{aligned} \tau_n \mathcal{G}(x_n, y_n) &\leq \langle x_{n+1} - z_{n+1}, \bar{x} - x_{n+1} \rangle + \psi \langle \bar{\theta}_n(x_n - z_{n+1}), x_{n+1} - x_n \rangle \\ &+ \frac{1}{\beta} \langle y_n - y_{n-1}, \bar{y} - y_n \rangle + \tau_n \langle K(x_n - x_{n+1}), y_n - y_{n-1} \rangle \\ &+ \tau_n \langle \nabla h(x_n) - \nabla h(x_{n-1}), x_n - x_{n+1} \rangle. \end{aligned} \quad (31)$$

Furthermore, using (19b) on the first three terms of the RHS of (31), we obtain

$$\begin{aligned} \tau_n \mathcal{G}(x_n, y_n) &+ \frac{1}{2} \|\bar{x} - x_{n+1}\|^2 + \frac{1}{2\beta} \|\bar{y} - y_n\|^2 \leq \frac{1}{2} \|\bar{x} - z_{n+1}\|^2 + \frac{1}{2\beta} \|\bar{y} - y_{n-1}\|^2 \\ &- \frac{1}{2} \|x_{n+1} - z_{n+1}\|^2 - \frac{\psi \bar{\theta}_n}{2} \|x_n - z_{n+1}\|^2 - \frac{\psi \bar{\theta}_n}{2} \|x_n - x_{n+1}\|^2 \\ &+ \frac{\psi \bar{\theta}_n}{2} \|x_{n+1} - z_{n+1}\|^2 - \frac{1}{2\beta} \|y_n - y_{n-1}\|^2 + \tau_n \langle K(x_n - x_{n+1}), y_n - y_{n-1} \rangle \\ &+ \langle \nabla h(x_n) - \nabla h(x_{n-1}), x_n - x_{n+1} \rangle. \end{aligned} \quad (32)$$

Now, using equation (22) along with the Cauchy-Schwarz inequality, we obtain

$$\begin{aligned} \tau_n \langle \nabla h(x_n) - \nabla h(x_{n-1}), x_n - x_{n+1} \rangle &\leq \tau_n \|\nabla h(x_n) - \nabla h(x_{n-1})\| \|x_n - x_{n+1}\| \\ &\leq \mu' \|x_n - x_{n-1}\| \|x_n - x_{n+1}\| \\ &\leq \frac{\mu'}{2} \|x_n - x_{n-1}\|^2 + \frac{\mu'}{2} \|x_n - x_{n+1}\|^2. \end{aligned} \quad (33)$$

In a similar manner, from (22), we have

$$\begin{aligned}
\tau_n \langle K(x_n - x_{n+1}), y_n - y_{n-1} \rangle &\leq \tau_n \|Kx_n - Kx_{n+1}\| \|y_n - y_{n-1}\| \\
&\leq \frac{\mu}{\sqrt{\beta}} \|x_n - x_{n+1}\| \|y_n - y_{n-1}\| \\
&\leq \frac{\mu}{2} \|x_n - x_{n+1}\|^2 + \frac{\mu}{2\beta} \|y_n - y_{n-1}\|^2.
\end{aligned} \tag{34}$$

Also, from equation (20), see that

$$\|\bar{x} - x_{n+1}\|^2 = \frac{\psi}{\psi - 1} \|\bar{x} - z_{n+2}\|^2 - \frac{1}{\psi - 1} \|\bar{x} - z_{n+1}\|^2 + \frac{1}{\psi} \|x_{n+1} - z_{n+1}\|^2. \tag{35}$$

Combining (32), (33), (34) and (35), we get

$$\begin{aligned}
2\tau_n \mathcal{G}(x_n, y_n) + \frac{\psi}{\psi - 1} \|\bar{x} - z_{n+2}\|^2 + \frac{1}{\beta} \|\bar{y} - y_n\|^2 &\leq \frac{\psi}{\psi - 1} \|\bar{x} - z_{n+1}\|^2 + \frac{1}{\beta} \|\bar{y} - y_{n-1}\|^2 \\
+ (\psi \bar{\theta}_n - 1 - \frac{1}{\psi}) \|x_{n+1} - z_{n+1}\|^2 - \psi \bar{\theta}_n \|x_n - z_{n+1}\|^2 + \mu' \|x_n - x_{n-1}\|^2 \\
- (\psi \bar{\theta}_n - \mu - \mu') \|x_n - x_{n+1}\|^2 - \left(\frac{1}{\beta} - \frac{\mu}{\beta}\right) \|y_n - y_{n-1}\|^2.
\end{aligned} \tag{36}$$

Noting the fact that (τ_n) is nonincreasing, we have

$$\psi \bar{\theta}_n - 1 - \frac{1}{\psi} \leq \psi - 1 - \frac{1}{\psi} \leq 0, \quad \forall \psi \in (1, \phi]. \tag{37}$$

From Proposition 3.4, we have $\lim_{n \rightarrow \infty} \psi \bar{\theta}_n - \mu - \mu' = \psi - \mu - \mu' > 2\mu - \mu - \mu' = \mu - \mu'$. So, there exists a natural number n_2 such that

$$\psi \bar{\theta}_n - \mu - \mu' > \mu - \mu', \quad \forall n \geq n_2. \tag{38}$$

Also, notice that $\mu < \frac{\psi}{2} < 1 \implies \left(\frac{1}{\beta} - \frac{\mu}{\beta}\right) > 0$. Combining equations (36), (37) and (38), $\forall n \geq n_2$, we obtain

$$\begin{aligned}
2\tau_n \mathcal{G}(x_n, y_n) + \frac{\psi}{\psi - 1} \|\bar{x} - z_{n+2}\|^2 + \frac{1}{\beta} \|\bar{y} - y_n\|^2 + (\mu - \mu') \|x_n - x_{n+1}\|^2 \\
\leq \frac{\psi}{\psi - 1} \|\bar{x} - z_{n+1}\|^2 + \frac{1}{\beta} \|\bar{y} - y_{n-1}\|^2 + \mu' \|x_n - x_{n-1}\|^2 - \psi \bar{\theta}_n \|x_n - z_{n+1}\|^2.
\end{aligned} \tag{39}$$

Since $\mu > 2\mu'$, it follows that $\mu - \mu' > \mu'$. Combining this result with (39), we derive Lemma 3.5. \square

Theorem 3.6. *Under Assumptions 2.2, 2.3, and 3.1, let $\{(z_n, x_n, \tau_n, y_n)\}$ be the sequence generated by Algorithm 2. Then $\{(x_n, y_n)\}$ converges to a solution of (5).*

Proof. Let (\bar{x}, \bar{y}) be a saddle point of \mathcal{L} . Then, from (17), it follows that $2\tau_n \mathcal{G}(x_n, y_n) \geq 0 \forall n$. Now, by Lemma 3.5, there exists a natural number n_2 such

that, $\forall n \geq n_2$, we have $p_{n+1} \leq p_n - q_n$, where

$$\begin{aligned} p_n &= \frac{\psi}{\psi - 1} \|\bar{x} - z_{n+1}\|^2 + \frac{1}{\beta} \|\bar{y} - y_{n-1}\|^2 + \mu' \|x_n - x_{n-1}\|^2, \\ q_n &= \psi \bar{\theta}_n \|x_n - z_{n+1}\|^2. \end{aligned} \quad (40)$$

From Lemma 2.5, we obtain $\lim_{n \rightarrow \infty} p_n \in \mathbb{R}$ and $\lim_{n \rightarrow \infty} q_n = 0$. This implies that $\lim_{n \rightarrow \infty} \psi \bar{\theta}_n \|x_n - z_{n+1}\|^2 = 0$. Furthermore, in Proposition 3.4, following the fact that $\lim_{n \rightarrow \infty} \tau_n = \tau \geq \eta$, we obtain

$$\lim_{n \rightarrow \infty} \|x_n - z_{n+1}\|^2 = \lim_{n \rightarrow \infty} \frac{1}{\psi^2} \|x_n - z_n\|^2 = 0. \quad (41)$$

Again, using (41) and the triangle inequality, we obtain

$$\lim_{n \rightarrow \infty} \|x_n - x_{n-1}\|^2 = 0. \quad (42)$$

Combining the fact that $\lim_{n \rightarrow \infty} p_n$ is finite with (41), we obtain that all the sequences $\{x_n\}$, $\{y_n\}$ and $\{z_n\}$ are bounded. Now suppose that (\tilde{x}, \tilde{y}) is a cluster point of $\{(x_n, y_n)\}$ and $\{(x_{n_k}, y_{n_k})\}$ is a subsequence of $\{(x_n, y_n)\}$ that converges to (\tilde{x}, \tilde{y}) , i.e., $\lim_{n \rightarrow \infty} x_{n_{k+1}} = \tilde{x}$, and $\lim_{n \rightarrow \infty} y_{n_k} = \tilde{y}$. Then, from equation (41), we obtain $\lim_{n \rightarrow \infty} z_{n_{k+1}} = \tilde{x}$. Using (21), (23), (27), (28) and, Lemma 2.1, $\forall (x, y) \in \mathbb{X} \times \mathbb{Y}$, we have

$$\begin{aligned} \langle x_{n_k} - z_{n_k} + \tau_{n_{k-1}} K^* y_{n_{k-1}} + \tau_{n_{k-1}} \nabla h(x_{n_{k-1}}), x - x_{n_k} \rangle &\geq \tau_{n_{k-1}} (f(x_{n_k}) - f(x)), \\ \left\langle \frac{1}{\beta} (y_{n_k} - y_{n_{k-1}}) + \tau_{n_k} K x_{n_k}, y - y_{n_{k-1}} \right\rangle &\geq \tau_{n_k} (g^*(y_{n_k}) - g^*(y)). \end{aligned}$$

Recalling that both f, g^* are lower-semi continuous and letting $k \rightarrow \infty$, we derive

$$\langle K^* \tilde{y} + \nabla h(\tilde{x}), x - \tilde{x} \rangle \geq f(\tilde{x}) - f(x) \quad \text{and} \quad \langle K \tilde{x}, y - \tilde{y} \rangle \geq g^*(\tilde{y}) - g^*(y). \quad (43)$$

Both the inequalities in (43) imply that (\tilde{x}, \tilde{y}) is a saddle point of (5). Now, putting $\bar{x} = \tilde{x}$ and $\bar{y} = \tilde{y}$ in (40), we obtain $\lim_{n \rightarrow \infty} p_{n_k} = 0$. Furthermore, $\lim_{n \rightarrow \infty} p_n$ exists, this implies that $\lim_{n \rightarrow \infty} p_n = 0$. Thus, we have $\lim_{n \rightarrow \infty} z_n = \tilde{x}$ and $\lim_{n \rightarrow \infty} y_n = \tilde{y}$. Again, by observing (41), we obtain $\lim_{n \rightarrow \infty} x_n = \tilde{x}$. This completes the proof. \square

Remark 3.7. Since (τ_n) is a nonincreasing sequence, if $\tau_0 \leq \min\{\frac{\mu}{\sqrt{\beta}\|K\|}, \frac{\mu'}{\bar{L}}\}$, then $\tau_n = \tau_0, \forall n$, i.e. (τ_n) is constant. Let $\tau_n = \tau_0 = \tau$. Then $\forall \psi \in (1, \phi]$, we have $\tau\sigma\|K\|^2 + 2\tau\bar{L} = \beta\tau^2\|K\|^2 + 2\tau\bar{L} \leq \mu^2 + 2\mu' < \frac{\psi^2}{4} + \frac{\psi}{2} < \psi$. Thus, we get the stepsize condition required for the global convergence of extended GRPDA [43] with fixed stepsize.

3.2. Extended convergence region of P-GRPDA

In [9, Theorem 2.1], the authors showed that the upper bound of the region of convergence for GRPDA (10) can be extended from the Golden Ratio ϕ to $1 + \sqrt{3}$.

Furthermore, they established the convergence of GRPDA under the following step-size condition: $\tau\sigma\|K\|^2 < \frac{\psi(2+2\psi-\psi^2)}{\psi+1}$, where $\psi \in (1, 1 + \sqrt{3})$. This stepsize is more relaxed compared to those required for both GRPDA (10) and the Chambolle–Pock primal-dual algorithm (9). In the following theorem, we also extend the convergence region of Algorithm 2 from $(1, \phi]$ to $(1, 1 + \sqrt{3})$.

Theorem 3.8. *Under Assumptions 2.2, 2.3, and 3.1, let the sequence $\{(z_n, x_n, \tau_n, y_n)\}$ be generated by Algorithm 2, where the parameters μ, μ' satisfy*

$$0 < 3\mu' < \mu < \frac{\psi}{2} + \frac{\psi(1 + \psi - \psi^2)}{2(\psi + 1)}, \quad \forall \psi \in (1, 1 + \sqrt{3}). \quad (44)$$

Then, $\{(x_n, y_n)\}$ converges to a solution of (5).

Proof. To prove this theorem, we proceed with the calculations as outlined in Lemma 3.5 up to the inequality (36). From this point, we claim the following inequality holds

$$\frac{\psi\bar{\theta}_n(1 + \psi - \psi^2\bar{\theta}_n)}{\psi + 1} \|x_{n+1} - x_n\|^2 \leq (1 + \frac{1}{\psi} - \psi\bar{\theta}_n) \|x_{n+1} - z_{n+1}\|^2 + \psi\bar{\theta}_n \|x_n - z_{n+1}\|^2. \quad (45)$$

To show this, we distinguish two cases based on the value of ψ : (i) $\psi \in (1, \phi]$ and (ii) $\psi \in (\phi, 1 + \sqrt{3})$. In the first case, using the fact that (τ_n) is nonincreasing, we have $1 + \frac{1}{\psi} - \psi\bar{\theta}_n \geq 1 + \frac{1}{\psi} - \psi \geq 0$, $\forall \psi \in (1, \phi]$. Now, by taking $p = 1 + \frac{1}{\psi} - \psi\bar{\theta}_n$, $q = \psi\bar{\theta}_n$, $m_1 = \|x_{n+1} - z_{n+1}\|$ and $m_2 = \|x_n - z_{n+1}\|$ in Lemma 2.6, and by noting that $\|x_{n+1} - x_n\|^2 \leq (m_1 + m_2)^2$, we obtain (45). Before proving the second case, notice that the extended bounds on μ, μ' and ψ in (44) do not change the result in Proposition 3.4, which indicates that (τ_n) is bounded below by η and that $\lim_{n \rightarrow \infty} \tau_n \geq \eta > 0$, $\forall \psi \in (1, 1 + \sqrt{3})$. Thus, for the second case $\psi \in (\phi, 1 + \sqrt{3})$, we have

$$\lim_{n \rightarrow \infty} \frac{\psi\bar{\theta}_n(\psi^2\bar{\theta}_n - \psi - 1)}{\psi + 1} = \frac{\psi(\psi^2 - \psi - 1)}{\psi + 1} > 0.$$

Hence, there exists a natural number k_3 such that $\frac{\psi\bar{\theta}_n(\psi^2\bar{\theta}_n - \psi - 1)}{\psi + 1} > 0$, $\forall n \geq k_3$. Now, by setting $p = \frac{\psi\bar{\theta}_n(\psi^2\bar{\theta}_n - \psi - 1)}{\psi + 1}$, $q = \psi\bar{\theta}_n$ with $m_1 = \|x_{n+1} - x_n\|$ and $m_2 = \|x_n - z_{n+1}\|$ in Lemma 2.6, and by noting the facts that $\|x_{n+1} - z_{n+1}\|^2 \leq (m_1 + m_2)^2$, and $\frac{pq}{p+q} = \frac{\psi^2\bar{\theta}_n - \psi - 1}{\psi}$, we obtain

$$\frac{\psi^2\bar{\theta}_n - \psi - 1}{\psi} \|x_{n+1} - z_{n+1}\|^2 \leq \frac{\psi\bar{\theta}_n(\psi^2\bar{\theta}_n - \psi - 1)}{\psi + 1} \|x_{n+1} - x_n\|^2 + \psi\bar{\theta}_n \|x_n - z_{n+1}\|^2. \quad (46)$$

Rearranging (46) gives us (45). Therefore, $\forall n \geq k_3$, substituting inequality (45) into (36), and from (44), observing the fact that $0 < \mu < 1$, $\forall \psi \in (1, 1 + \sqrt{3})$, we obtain

$$\begin{aligned}
2\tau_n \mathcal{G}(x_n, y_n) + \frac{\psi}{\psi-1} \|\bar{x} - z_{n+2}\|^2 + \frac{1}{\beta} \|y - y_n\|^2 &\leq \frac{\psi}{\psi-1} \|\bar{x} - z_{n+1}\|^2 + \frac{1}{\beta} \|y - y_{n-1}\|^2 \\
- \left(\frac{\psi \bar{\theta}_n (1 + \psi - \psi^2 \bar{\theta}_n)}{\psi + 1} + \psi \bar{\theta}_n - \mu - \mu' \right) \|x_{n+1} - x_n\|^2 + \mu' \|x_n - x_{n-1}\|^2 &\quad (47)
\end{aligned}$$

Recalling that Proposition 3.4 holds for $\psi, \mu, \mu' > 0$, we deduce that $\lim_{n \rightarrow \infty} \bar{\theta}_n = 1$. Furthermore, from (44) and (47), we have

$$\begin{aligned}
\lim_{n \rightarrow \infty} \left(\frac{\psi \bar{\theta}_n (1 + \psi - \psi^2 \bar{\theta}_n)}{\psi + 1} + \psi \bar{\theta}_n - \mu - \mu' \right) &= \frac{\psi(1 + \psi - \psi^2)}{\psi + 1} + \psi - \mu - \mu' \\
&> 2\mu - \mu - \mu' \\
&= \mu - \mu' > 2\mu' \quad \text{as } 3\mu' < \mu.
\end{aligned}$$

Therefore, there exists a natural number k_4 such that, $\forall n \geq k_4$, the following holds

$$\frac{\psi \bar{\theta}_n (1 + \psi - \psi^2 \bar{\theta}_n)}{\psi + 1} + \psi \bar{\theta}_n - \mu - \mu' > 2\mu'. \quad (48)$$

Let $k_5 = \max\{k_3, k_4\}$. Then, $\forall n \geq k_5$, combining (47) and (48), we get

$$\begin{aligned}
2\tau_n \mathcal{G}(x_n, y_n) + \frac{\psi}{\psi-1} \|\bar{x} - z_{n+2}\|^2 + \frac{1}{\beta} \|\bar{y} - y_n\|^2 + \mu' \|x_{n+1} - x_n\|^2 \\
\leq \frac{\psi}{\psi-1} \|\bar{x} - z_{n+1}\|^2 + \frac{1}{\beta} \|\bar{y} - y_{n-1}\|^2 + \mu' \|x_n - x_{n-1}\|^2 - \mu' \|x_n - x_{n+1}\|^2. \quad (49)
\end{aligned}$$

Let (\bar{x}, \bar{y}) be a saddle point of \mathcal{L} . Then, from (17), we have $2\tau_n \mathcal{G}(x_n, y_n) \geq 0 \quad \forall n$. Again, inequality (49) can be written as $p_{n+1} \leq p_n - q_n, \forall n \geq k_5$, where

$$\begin{aligned}
p_n &= \frac{\psi}{\psi-1} \|\bar{x} - z_{n+1}\|^2 + \frac{1}{\beta} \|\bar{y} - y_{n-1}\|^2 + \mu' \|x_n - x_{n-1}\|^2, \\
q_n &= \mu' \|x_n - x_{n+1}\|^2.
\end{aligned} \quad (50)$$

From (49), (50), and using Lemma 2.5, we obtain $\sum_{n=1}^{\infty} \|x_n - x_{n-1}\|^2 < \infty$. To complete the proof, it remains to show that $\lim_{n \rightarrow \infty} \|x_n - z_n\| = 0$. Once this is established, the rest of the proof follows from Theorem 3.6. By using (20), we have

$$\begin{aligned}
\|x_n - z_n\| &\leq \frac{\psi-1}{\psi} \|x_n - x_{n-1}\| + \frac{1}{\psi} \|x_n - z_{n-1}\| \\
&\leq \frac{\psi-1}{\psi} \|x_n - x_{n-1}\| + \frac{1}{\psi} \|x_n - x_{n-1}\| + \frac{1}{\psi} \|x_{n-1} - z_{n-1}\| \\
&= \frac{1}{\psi} \|x_{n-1} - z_{n-1}\| + \|x_n - x_{n-1}\|.
\end{aligned} \quad (51)$$

Again, using the facts $\sum_{n=1}^{\infty} \|x_n - x_{n-1}\|^2 < \infty$ and $\frac{1}{\psi} < 1 \quad \forall \psi \in (1, 1 + \sqrt{3})$, it follows from (51) that $\sum_{n=1}^{\infty} \|x_n - z_n\|^2 < \infty$. Consequently, we have $\lim_{n \rightarrow \infty} \|x_n - z_n\| = 0$.

Hence, the proof is concluded. \square

Remark 3.9. Figure 1 shows the largest values of μ and μ' that satisfies $0 < 3\mu' < \mu < f_1(\psi)$, where $f_1(\psi) = \frac{\psi}{2} + \frac{\psi(1+\psi-\psi^2)}{2(\psi+1)}$, and $\psi \in (1, 1 + \sqrt{3})$.

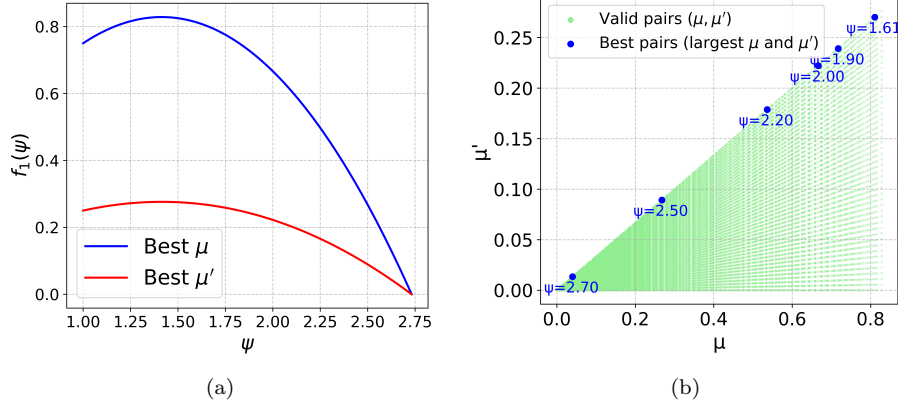


Figure 1. (a) Largest values of μ and μ' for a given ψ . (b) Valid pairs of μ and μ' and some best pairs for $\psi = 1.618, 1.90, 2.0, 2.20, 2.50$ and 2.70 .

4. Convergence rate

In this section, we establish the ergodic sublinear rate of convergence of Algorithm 2 and R-linear convergence rate when h and g^* are strongly convex functions.

Theorem 4.1. (Sublinear rate of convergence) Under Assumptions 2.2, 2.3 and 3.1, let $\{(z_n, x_n, y_n, \tau_n)\}$ be the sequence generated by Algorithm 2, and suppose that (\bar{x}, \bar{y}) is a saddle point of \mathcal{L} . Then, there exists a natural number n_2 such that the following holds

$$\mathcal{G}(\tilde{x}_N, \tilde{y}_N) \leq \frac{1}{2\eta N} \left(\frac{\psi}{\psi-1} \|\bar{x} - z_{n_2+1}\|^2 + \frac{1}{\beta} \|\bar{y} - y_{n_2-1}\|^2 + \mu' \|x_{n_2} - x_{n_2-1}\|^2 \right), \quad (52)$$

where $N \geq 1$, $\eta = \min \left\{ \tau_0, \frac{\mu}{\sqrt{\beta}\|K\|}, \frac{\mu'}{L} \right\}$, and

$$\tilde{x}_N = \frac{1}{N} \sum_{n=n_2+1}^{n_2+N} x_n, \quad \tilde{y}_N = \frac{1}{N} \sum_{n=n_2+1}^{n_2+N} y_n.$$

Proof. It follows from (26) and the definition of q_n that

$$2\tau_n \mathcal{G}(x_n, y_n) \leq p_n - p_{n+1}, \quad \forall n \geq n_2.$$

We know that $\tau_n \geq \eta, \forall n$. This implies that

$$2\eta \mathcal{G}(x_n, y_n) \leq 2\tau_n \mathcal{G}(x_n, y_n) \leq p_n - p_{n+1}, \quad \forall n \geq n_2. \quad (53)$$

By taking summation over $n = n_2 + 1, \dots, n_2 + N$, we obtain

$$\begin{aligned} 2\eta \sum_{n=n_2+1}^{n_2+N} \mathcal{G}(x_n, y_n) &\leq p_{n_2} - p_{n_2+N} \\ &\leq p_{n_2} = \frac{\psi}{\psi-1} \|\bar{x} - z_{n_2+1}\|^2 + \frac{1}{\beta} \|\bar{y} - y_{n_2-1}\|^2 + \mu' \|x_{n_2} - x_{n_2-1}\|^2. \end{aligned} \quad (54)$$

Again, using the definition of \tilde{x}_N, \tilde{y}_N along with convexity of $\mathcal{L}(x, y)$ in x variable and concavity in y variable, we have

$$\begin{aligned} \mathcal{G}(\tilde{x}_N, \tilde{y}_N) &= \mathcal{L}(\tilde{x}_N, \bar{y}) - \mathcal{L}(\bar{x}, \tilde{y}_N) \\ &\leq \frac{1}{N} \sum_{n=n_2+1}^{n_2+N} \mathcal{L}(x_n, \bar{y}) - \mathcal{L}(\bar{x}, y_n) \\ &= \frac{1}{N} \sum_{n=n_2+1}^{n_2+N} \mathcal{G}(x_n, y_n) \leq \frac{p_{n_2}}{2N\eta}. \end{aligned} \quad (55)$$

This proves our assertion. \square

4.1. Nonergodic rate of convergence

In this section, we prove the R-linear rate of convergence for Algorithm 2 when h and g^* are strongly convex functions. First, let us recall the definition of linear convergence of a sequence. Given a sequence $(v_n) \in \mathbb{X}$ we say that the sequence (v_n) converges Q-linearly to $v \in \mathbb{X}$ if there exists $q \in (0, 1)$ and a natural number k such that $\|v_{n+1} - v\| \leq q \|v_n - v\|$ for all $n \geq k$. Furthermore, we say (v_n) converges R-linearly to v if there exists a sequence ϵ_n and a natural number k_1 such that $\|v_n - v\| \leq \epsilon_n$ for all $n \geq k_1$ and ϵ_n converges Q-linearly to 0.

Given a differentiable function h , we say that h is strongly convex if there exist a constant $\gamma_h > 0$ such that

$$h(y) - h(z) \geq \langle \nabla h(z), y - z \rangle + \frac{\gamma_h}{2} \|y - z\|^2, \quad \forall y, z \in \mathbb{X}. \quad (56)$$

Furthermore, for a nonsmooth function g^* , we call g^* to be strongly convex if there exist a constant $\gamma_{g^*} > 0$ such that

$$g^*(y) - g^*(z) \geq \langle u, y - z \rangle + \frac{\gamma_{g^*}}{2} \|y - z\|^2, \quad \forall y, z \in \mathbb{Y}, \quad \forall u \in \partial g^*(z). \quad (57)$$

Assumption 4.2. *Suppose that g^*, h are strongly convex functions with constants $\gamma_{g^*}, \gamma_h > 0$ respectively.*

Theorem 4.3. *Under Assumptions 2.2, 2.3 and 4.2, let $\{(x_n, y_n)\}$ be the sequences generated by Algorithm 2. Suppose that $\{(x_n, y_n)\}$ converges to the unique primal-dual solution (\bar{x}, \bar{y}) . Then, there exist constants $V_1, V_2, Z > 0$, a scalar $\zeta \in (0, 1)$, and a*

natural number n_4 such that

$$\|\bar{x} - z_{n+2}\|^2 \leq Z\zeta^n, \quad \|\bar{y} - y_n\|^2 \leq V_1\zeta^n, \quad \|x_n - x_{n+1}\|^2 \leq V_2\zeta^n, \quad \forall n \geq n_4, \quad (58)$$

and thus $\{(x_n, y_n)\}$ converges R -linearly to zero.

Proof. From the dual update (23) in Algorithm 2, we have

$$y_{n-1} - y_n + \sigma_n K x_n \in \sigma_n \partial g^*(y_n). \quad (59)$$

Using (59) along with the definition of strong convexity of g^* in (57), and the fact $\sigma_n = \beta\tau_n$, we obtain

$$\tau_n(g^*(y_n) - g^*(\bar{y})) \leq \left\langle \frac{1}{\beta}(y_n - y_{n-1}) - \tau_n K x_n, \bar{y} - y_n \right\rangle - \frac{\tau_n \gamma g^*}{2} \|\bar{y} - y_n\|^2. \quad (60)$$

Again, from (30) and (60), we derive

$$\begin{aligned} \tau_n(\mathcal{L}(x_n, \bar{y}) - \mathcal{L}(\bar{x}, y_n)) &\leq \langle x_{n+1} - z_{n+1}, \bar{x} - x_{n+1} \rangle + \psi \langle \bar{\theta}_n(x_n - z_{n+1}), x_{n+1} - x_n \rangle \\ &+ \left\langle \frac{1}{\beta}(y_n - y_{n-1}), \bar{y} - y_n \right\rangle + \langle K(x_n - x_{n+1}), y_n - y_{n-1} \rangle + \tau_n \langle \nabla h(x_{n-1}), x_{n+1} - x_n \rangle \\ &+ \tau_n(h(x_n) - h(\bar{x}) + \tau_n \langle \nabla h(x_n), \bar{x} - x_{n+1} \rangle) - \frac{\tau_n \gamma g^*}{2} \|\bar{y} - y_n\|^2. \end{aligned} \quad (61)$$

Furthermore, using (56), and the definition of $\mathcal{G}(x_n, y_n)$, we have

$$\begin{aligned} \tau_n \mathcal{G}(x_n, y_n) &\leq \langle x_{n+1} - z_{n+1}, \bar{x} - x_{n+1} \rangle + \psi \langle \bar{\theta}_n(x_n - z_{n+1}), x_{n+1} - x_n \rangle \\ &+ \frac{1}{\beta} \langle y_n - y_{n-1}, \bar{y} - y_n \rangle + \tau_n \langle K(x_n - x_{n+1}), y_n - y_{n-1} \rangle \\ &+ \tau_n \langle \nabla h(x_n) - \nabla h(x_{n-1}), x_n - x_{n+1} \rangle - \frac{\tau_n \gamma g^*}{2} \|\bar{y} - y_n\|^2 - \frac{\gamma h \tau_n}{2} \|\bar{x} - x_n\|^2. \end{aligned} \quad (62)$$

Doing similar calculations as in Lemma 3.5, and following (37), (38), there exists a natural number n_2 such that $\forall n \geq n_2$

$$\begin{aligned} 2\tau_n \mathcal{G}(x_n, y_n) &+ \frac{\psi}{\psi - 1} \|\bar{x} - z_{n+2}\|^2 + \frac{1}{\beta} \|\bar{y} - y_n\|^2 + (\mu - \mu') \|x_n - x_{n+1}\|^2 \\ &\leq \frac{\psi}{\psi - 1} \|\bar{x} - z_{n+1}\|^2 + \frac{1}{\beta} \|\bar{y} - y_{n-1}\|^2 + \mu' \|x_n - x_{n-1}\|^2 - \psi \bar{\theta}_n \|x_n - z_{n+1}\|^2 \\ &\quad - \gamma h \tau_n \|\bar{x} - x_n\|^2 - \tau_n \gamma g^* \|\bar{y} - y_n\|^2. \end{aligned} \quad (63)$$

Since (\bar{x}, \bar{y}) is a primal-dual solution of (1). Therefore, from (17), we have $\mathcal{G}(x_n, y_n) \geq 0$ for all n . Again, from the fact (τ_n) is convergent and converges to a positive constant, it follows that

$$\lim_{n \rightarrow \infty} \psi \bar{\theta}_n = \psi > 4\mu'.$$

Thus, there exists a natural number n_3 such that

$$\psi\bar{\theta}_n > 4\mu', \quad \forall n \geq n_3.$$

Consequently, taking $n_4 = \max\{n_2, n_3\}$, from (63), $\forall n \geq n_4$, we obtain

$$\begin{aligned} \frac{\psi}{\psi-1}\|\bar{x} - z_{n+2}\|^2 + \frac{1}{\beta}\|\bar{y} - y_n\|^2 + (\mu - \mu')\|x_n - x_{n+1}\|^2 &\leq \frac{\psi}{\psi-1}\|\bar{x} - z_{n+1}\|^2 \\ &+ \frac{1}{\beta}\|y - y_{n-1}\|^2 + \mu'\|x_n - x_{n-1}\|^2 - 4\mu'\|x_n - z_{n+1}\|^2 \\ &- \gamma_h\tau_n\|\bar{x} - x_n\|^2 - \tau_n\gamma_{g^*}\|\bar{y} - y_n\|^2. \end{aligned} \quad (64)$$

The strong convexity of h and Lipschitz continuity of ∇h implies that $0 < \gamma_h \leq \bar{L}$. Consequently, it follows that $0 < 2\eta\gamma_h \leq 2\bar{L}\frac{\mu'}{L} = 2\mu'$, where $\eta = \min\left\{\tau_0, \frac{\mu}{\sqrt{\beta}\|K\|}, \frac{\mu'}{L}\right\}$, as defined in Proposition 3.4. Furthermore, using this fact, we obtain

$$\begin{aligned} \gamma_h\tau_n\|\bar{x} - x_n\|^2 + 4\mu'\|x_n - z_{n+1}\|^2 &\geq \eta\gamma_h\|\bar{x} - x_n\|^2 + 2\mu'\|x_n - z_{n+1}\|^2 \\ &\geq \eta\gamma_h(\|\bar{x} - x_n\|^2 + \|x_n - z_{n+1}\|^2) \\ &\geq \eta\gamma_h\|\bar{x} - z_{n+1}\|^2. \end{aligned} \quad (65)$$

Combining (64) and (65), we have

$$\begin{aligned} \frac{\psi}{\psi-1}\|\bar{x} - z_{n+2}\|^2 + \left(\frac{1}{\beta} + \tau_n\gamma_{g^*}\right)\|\bar{y} - y_n\|^2 + (2\mu - \mu')\|x_n - x_{n+1}\|^2 \\ \leq \left(\frac{\psi}{\psi-1} - \eta\gamma_h\right)\|\bar{x} - z_{n+1}\|^2 + \frac{1}{\beta}\|\bar{y} - y_{n-1}\|^2 + \mu'\|x_n - x_{n-1}\|^2. \end{aligned} \quad (66)$$

Rearranging all the terms, we obtain

$$\begin{aligned} \|\bar{x} - z_{n+2}\|^2 + \frac{\psi-1}{\psi}\left(\frac{1}{\beta} + \eta\gamma_{g^*}\right)\|\bar{y} - y_n\|^2 + \frac{\psi-1}{\psi}(\mu - \mu')\|x_n - x_{n+1}\|^2 \\ \leq \left(1 - \frac{\psi-1}{\psi}\eta\gamma_h\right)\|\bar{x} - z_{n+1}\|^2 + \frac{1}{\beta}\frac{\psi-1}{\psi}\|\bar{y} - y_{n-1}\|^2 + \mu'\frac{\psi-1}{\psi}\|x_n - x_{n-1}\|^2. \end{aligned} \quad (67)$$

Now, take $\zeta = \max\left\{1 - \frac{\psi-1}{\psi}\eta\gamma_h, \frac{\mu'}{\mu - \mu'}, \frac{1}{1 + \beta\eta\gamma_{g^*}}\right\}$, then $\zeta \in (0, 1)$ and it follows from (67) that, $\forall n \geq n_4$

$$\begin{aligned} \|\bar{x} - z_{n+2}\|^2 + \frac{\psi-1}{\psi}\left(\frac{1}{\beta} + \eta\gamma_{g^*}\right)\|\bar{y} - y_n\|^2 + \frac{\psi-1}{\psi}(\mu - \mu')\|x_n - x_{n+1}\|^2 \\ \leq \zeta \left(\|\bar{x} - z_{n+1}\|^2 + \frac{\psi-1}{\psi}\left(\frac{1}{\beta} + \eta\gamma_{g^*}\right)\|\bar{y} - y_{n-1}\|^2 + \frac{\psi-1}{\psi}(\mu - \mu')\|x_n - x_{n-1}\|^2 \right). \end{aligned} \quad (68)$$

Iterating (68), it follows that

$$\begin{aligned} \|\bar{x} - z_{n+2}\|^2 + \frac{\psi - 1}{\psi} \left(\frac{1}{\beta} + \eta\gamma_{g^*} \right) \|\bar{y} - y_n\|^2 + \frac{\psi - 1}{\psi} (\mu - \mu') \|x_n - x_{n+1}\|^2 \\ \leq \zeta^{n-n_4+1} M, \quad \forall n \geq n_4 \end{aligned} \quad (69)$$

$$\begin{aligned} \text{where } M = \|\bar{x} - z_{n_4+1}\|^2 + \frac{\psi - 1}{\psi} \left(\frac{1}{\beta} + \eta\gamma_{g^*} \right) \|\bar{y} - y_{n_4-1}\|^2 \\ + \frac{\psi - 1}{\psi} (\mu - \mu') \|x_{n_4} - x_{n_4-1}\|^2. \end{aligned}$$

Moreover, setting $Z = \frac{M}{\zeta^{n_4-1}}$, we obtain

$$\begin{aligned} \|\bar{x} - z_{n+2}\|^2 + \frac{\psi - 1}{\psi} \left(\frac{1}{\beta} + \eta\gamma_{g^*} \right) \|\bar{y} - y_n\|^2 + \frac{\psi - 1}{\psi} (\mu - \mu') \|x_n - x_{n+1}\|^2 \\ \leq \zeta^n Z \quad \forall n \geq n_4. \end{aligned} \quad (70)$$

Therefore, (70) implies that $\|\bar{x} - z_{n+1}\|^2 + \frac{\psi - 1}{\psi} \left(\frac{1}{\beta} + \eta\gamma_{g^*} \right) \|\bar{y} - y_{n-1}\|^2 + \frac{\psi - 1}{\psi} (\mu - \mu') \|x_n - x_{n-1}\|^2$ converges R-Linearly to zero. Furthermore, from (70), $\forall n \geq n_4$, we also have

$$\|\bar{x} - z_{n+2}\|^2 \leq Z\zeta^n, \quad \|\bar{y} - y_n\|^2 \leq V_1\zeta^n, \quad \text{where } V_1 = \frac{\beta(\psi - 1)Z}{\psi(1 + \beta\eta\gamma_{g^*})}.$$

Since $\psi > 1 \forall \psi$, it follows that $V_1 > 0$. Furthermore, from (70), we obtain

$$\|x_n - x_{n+1}\|^2 \leq V_2\zeta^n, \quad \text{where } V_2 = \frac{\psi Z}{(\psi - 1)(\mu - \mu')}.$$

Since $\mu - \mu' > \mu > 0$, we have $V_2 > 0$ and thus $\|x_n - x_{n+1}\| \leq \sqrt{V_2}\zeta^{n/2}$. Now, for $m > n \geq n_4$, applying the triangle inequality gives

$$\begin{aligned} \|x_n - x_m\| &\leq \|x_n - x_{n+1}\| + \|x_{n+1} - x_{n+2}\| + \dots + \|x_{m-1} - x_m\| \\ &\leq \sqrt{V_2} \left(\zeta^{n/2} + \zeta^{(n+1)/2} + \dots + \zeta^{(m-1)/2} \right) \\ &\leq \sqrt{V_2}\zeta^{n/2} \left(\zeta + \zeta^{1/2} + \dots + \zeta^{m-n-1/2} \right) \\ &= \sqrt{V_2}\zeta^{n/2} \frac{1 - \zeta^{m-n/2}}{1 - \zeta^{1/2}}. \end{aligned} \quad (71)$$

Since $\zeta \in (0, 1)$, it follows from (71) that $\|x_n - x_m\| \leq \frac{\sqrt{V_2}\zeta^{n/2}}{1 - \zeta^{1/2}}$, $\forall m, n \geq n_4$. This proves that (x_n) is a Cauchy sequence. Moreover, it follows that (x_n) converges to \bar{x} . Finally, letting $m \rightarrow \infty$, we obtain $\|x_n - \bar{x}\| \leq \frac{\sqrt{V_2}\zeta^{n/2}}{1 - \zeta^{1/2}}$ for all $n \geq n_4$. This completes our proof. \square

5. The Adaptive extended Golden Ratio primal-dual algorithm

In this section, motivated by [21,37], we propose a fully adaptive version of E-GRPDA, namely aEGRPDA, which also does not rely on linesearch techniques to remove the dependency on $\|K\|$ and uses the local curvature information of ∇h to prove the global convergence. It was shown in [21] that aGRAAL for monotone variational inequality converges at $\mathcal{O}(1/N)$ rate. A similar result is also derived in this section. Next, for $n \geq 1$, we define

$$\bar{L}_n = \frac{\|\nabla h(x_n) - \nabla h(x_{n-1})\|}{\|x_n - x_{n-1}\|} \quad \text{and} \quad L_n = \frac{\|Kx_n - Kx_{n-1}\|}{\|x_n - x_{n-1}\|}.$$

Algorithm 3 The aEGRPDA for (12)

- 1: **Step 0:** Let $x_0 \in \mathbb{X}$, $y_0 \in \mathbb{Y}$, and define $z_0 = x_0$. Consider $\beta > 0$, $\psi \in (1, \phi]$, $\rho \in \left[1, \frac{1}{\psi} + \frac{1}{\psi^2}\right]$, $\theta_0 > 0$, and $\tau_{\max} \gg 0$. Suppose $\tau_0 > 0$ and $n \geq 1$.
- 2: **Step 1:** *Compute:*

$$\begin{aligned} z_n &= \frac{\psi - 1}{\psi} x_{n-1} + \frac{1}{\psi} z_{n-1}, \\ x_n &= \text{prox}_{\tau_{n-1}f}(z_n - \tau_{n-1}K^*y_{n-1} - \tau_{n-1}\nabla h(x_{n-1})). \end{aligned}$$

- 3: **Step 2:** *Update:*

$$\begin{aligned} \tau_n &= \min \left\{ \rho\tau_{n-1}, \frac{\psi\theta_{n-1}}{4(\bar{L}_n^2 + \beta\psi L_n^2)} \frac{1}{\tau_{n-1}}, \tau_{\max} \right\}, \\ \sigma_n &= \beta\tau_n. \end{aligned} \tag{72}$$

- 4: **Step 3:** *Compute:*

$$y_n = \text{prox}_{\sigma_n g^*}(y_{n-1} + \sigma_n Kx_n).$$

- 5: **Step 4:** *Update:* $\theta_n = \frac{\psi\tau_n}{\tau_{n-1}}$.
 - 6: **Step 5:** Let $n \leftarrow n + 1$ and return to Step 1.
-

Before we delve into the convergence analysis of Algorithm 3, some comments are in order.

Remark 5.1. In Algorithm 3, τ_{\max} is chosen to be a large value. In practice, we take $\tau_{\max} = 10^7$ and $\rho = \frac{1}{\psi} + \frac{1}{\psi^2}$ for a given ψ . As in Algorithm 2, we also adopt the convention $\frac{0}{0} = \infty$. Under this convention, $\tau_n = \min\{\rho\tau_{n-1}, \tau_{\max}\}$, when both $\nabla h(x_n) = \nabla h(x_{n-1})$ and $Kx_n = Kx_{n-1}$ holds for some n . Again, when $x_n \neq x_{n-1}$ but $\nabla h(x_n) = \nabla h(x_{n-1})$ and $Kx_n \neq Kx_{n-1}$ holds for some n , by adopting the convention $\frac{1}{0} = \infty$, we calculate τ_n as $\tau_n = \min\{\rho\tau_{n-1}, \frac{\theta_{n-1}}{4\beta\tau_{n-1}L_n^2}, \tau_{\max}\}$. Similarly, for the other case, following the same convention, τ_n is computed as $\tau_n = \min\{\rho\tau_{n-1}, \frac{\psi\theta_{n-1}}{4\tau_{n-1}L_n^2}, \tau_{\max}\}$.

Remark 5.2. The E-GRPDA algorithm (12) converges under the stepsize condition

$\tau\sigma\|K\|^2 + 2\tau\bar{L} < \psi$ for any $\psi \in (1, \phi]$, where $\sigma = \beta\tau$. Now, substituting the value of σ back into the stepsize inequality gives

$$\beta\tau^2\|K\|^2 + 2\tau\bar{L} < \psi \implies \beta\|K\|^2 + \frac{2\bar{L}}{\tau} - \frac{\psi}{\tau^2} < 0.$$

Solving this, we get, $\tau \in \left(0, \frac{\psi}{\bar{L} + \sqrt{\bar{L}^2 + \psi\beta\|K\|^2}}\right)$.

We show that Algorithm 3 converges when these estimates are satisfied locally given by $\tau_n \in \left(0, \frac{\psi}{2\sqrt{\bar{L}_n^2 + \psi\beta L_n^2}}\right)$ for any $\psi \in (1, \phi]$. In particular, we analyse the convergence of Algorithm 3 when $\tau_n\tau_{n-2} \leq \frac{\psi^2}{4(\bar{L}_n^2 + \psi\beta L_n^2)}$. This inequality implies that

$$\tau_n \leq \frac{\psi}{4(\bar{L}_n^2 + \psi\beta L_n^2)} \frac{\psi\tau_{n-1}}{\tau_{n-2}} \frac{1}{\tau_{n-1}} = \frac{\psi\theta_{n-1}}{4(\bar{L}_n^2 + \psi\beta L_n^2)} \frac{1}{\tau_{n-1}}, \quad \forall n \geq 1, \quad (73)$$

where $\tau_0, \theta_0 > 0$ and $\theta_n = \frac{\psi\tau_n}{\tau_{n-1}}$.

Remark 5.3. From equation (72), notice that

$$\tau_n \leq \frac{\theta_n\theta_{n-1}}{4\tau_n} \frac{1}{\bar{L}_n^2 + \beta\psi L_n^2} \quad \text{as} \quad \frac{\psi\theta_{n-1}}{\tau_{n-1}} = \frac{\theta_n\theta_{n-1}}{\tau_n}.$$

Therefore, it follows that $\tau_n^2\bar{L}_n^2 \leq \frac{\theta_n\theta_{n-1}}{4}$ or $\tau_n\bar{L}_n \leq \frac{\sqrt{\theta_n\theta_{n-1}}}{2}$. Similarly, from (72), we also derive $\tau_n L_n \leq \frac{1}{2}\sqrt{\frac{\theta_n\theta_{n-1}}{\beta\psi}}$.

Proposition 5.4. *Suppose that h is locally smooth and the sequence (x_n) generated by Algorithm 3 is bounded. Then, the sequences (τ_n) and (θ_n) are bounded below by positive constants.*

Proof. Since the sequence (x_n) is bounded, there exist a constant $\bar{L} > 0$ such that $\|\nabla h(x_n) - \nabla h(x_{n-1})\| \leq \bar{L}\|x_n - x_{n-1}\| \forall n$. Again, the existence of $\|K\|$ implies that $\|Kx_n - Kx_{n-1}\| \leq \|K\|\|x_n - x_{n-1}\| \forall n$. Thereafter, doing a similar calculation as in [33, Lemma 4.2], we derive

$$\tau_n \geq \frac{\psi}{4(\|K\|^2 + \beta\psi L^2)} \frac{1}{\tau_{\max}} \quad \text{and} \quad \theta_n \geq \frac{\psi^2}{4(\bar{L}^2 + \beta\psi\|K\|^2)} \frac{1}{\tau_{\max}^2} \quad \forall n.$$

□

Assumption 5.5. *Suppose that f and g are proper, convex and lower semicontinuous. The function $h : \mathbb{Y} \rightarrow \mathbb{R}$ is convex and locally smooth, i.e., for all compact set D , where $D \subset \mathbb{Y}$, there exists $L_D > 0$ such that*

$$\|\nabla h(x) - \nabla h(y)\| \leq \bar{L}_D\|x - y\|, \quad \forall x, y \in D.$$

Lemma 5.6. *Under Assumptions 2.2, 2.3, and 5.5, let $\{(z_n, x_n, y_n, \tau_n)\}$ be the sequence generated by Algorithm 3. Suppose that $(x^*, y^*) \in \Omega$ is a saddle point. Then the following holds as $n \geq 1$*

$$\begin{aligned} & 2\tau_n \mathcal{G}(x_n, y_n) + \frac{\psi}{\psi-1} \|x^* - z_{n+2}\|^2 + \frac{1}{\beta} \|y - y_n\|^2 + \frac{\theta_n}{4} \|x_n - x_{n+1}\|^2 \\ & \leq \frac{\psi}{\psi-1} \|x^* - z_{n+1}\|^2 + \frac{1}{\beta} \|y^* - y_{n-1}\|^2 + \frac{\theta_{n-1}}{4} \|x_n - x_{n-1}\|^2 - \theta_n \|x_n - z_{n+1}\|^2. \end{aligned} \quad (74)$$

Proof. Following the same arguments as in Lemma 3.5, we obtain

$$\begin{aligned} & 2\tau_n \mathcal{G}(x_n, y_n) + \|x^* - x_{n+1}\|^2 + \frac{1}{\beta} \|y^* - y_n\|^2 \leq \|x^* - z_{n+1}\|^2 \\ & + \frac{1}{\beta} \|y^* - y_{n-1}\|^2 - \|x_{n+1} - z_{n+1}\|^2 - \theta_n \|x_n - z_{n+1}\|^2 - \theta_n \|x_n - x_{n+1}\|^2 \\ & + \theta_n \|x_{n+1} - z_{n+1}\|^2 - \frac{1}{\beta} \|y_n - y_{n-1}\|^2 + \tau_n \langle Kx_n - Kx_{n+1}, y_n - y_{n-1} \rangle \\ & + \tau_n \langle \nabla h(x_n) - \nabla h(x_{n-1}), x_n - x_{n+1} \rangle. \end{aligned} \quad (75)$$

Using Cauchy-Schwarz inequality and Remark 5.3, we obtain

$$\begin{aligned} \tau_n \langle \nabla h(x_n) - \nabla h(x_{n-1}), x_n - x_{n+1} \rangle & \leq \tau_n \|\nabla h(x_n) - \nabla h(x_{n-1})\| \|x_n - x_{n+1}\| \\ & \leq \tau_n \bar{L}_n \|x_n - x_{n-1}\| \|x_n - x_{n+1}\| \\ & \leq \frac{\sqrt{\theta_n \theta_{n-1}}}{2} \|x_n - x_{n-1}\| \|x_n - x_{n+1}\| \\ & \leq \frac{\theta_n}{4} \|x_n - x_{n+1}\|^2 + \frac{\theta_{n-1}}{4} \|x_n - x_{n-1}\|^2. \end{aligned} \quad (76)$$

Similarly, we have

$$\begin{aligned} \tau_n \langle Kx_n - Kx_{n+1}, y_n - y_{n-1} \rangle & \leq \tau_n \|Kx_n - Kx_{n+1}\| \|y_n - y_{n-1}\| \\ & \leq \tau_n L_n \|x_n - x_{n+1}\| \|y_n - y_{n-1}\| \\ & \leq \frac{1}{2} \sqrt{\frac{\theta_n \theta_{n-1}}{\beta \psi}} \|x_n - x_{n+1}\| \|y_n - y_{n-1}\| \\ & \leq \frac{\theta_n}{4} \|x_n - x_{n+1}\|^2 + \frac{\theta_{n-1}}{2\beta \psi} \|y_n - y_{n-1}\|^2. \end{aligned} \quad (77)$$

Now, combining (75), (76), (77), and (35), we derive

$$\begin{aligned} & 2\tau_n \mathcal{G}(x_n, y_n) + \frac{\psi}{\psi-1} \|x^* - z_{n+2}\|^2 + \frac{1}{\beta} \|y^* - y_n\|^2 \leq \frac{\psi}{\psi-1} \|x^* - z_{n+1}\|^2 \\ & + \frac{1}{\beta} \|y^* - y_{n-1}\|^2 + (\theta_n - 1 - \frac{1}{\psi}) \|x_{n+1} - z_{n+1}\|^2 - \theta_n \|x_n - z_{n+1}\|^2 + \frac{\theta_{n-1}}{4} \|x_n - x_{n-1}\|^2 \\ & - (\theta_n - \frac{\theta_n}{4} - \frac{\theta_n}{4}) \|x_n - x_{n+1}\|^2 - \left(\frac{1}{\beta} - \frac{\theta_{n-1}}{2\beta \psi} \right) \|y_n - y_{n-1}\|^2. \end{aligned} \quad (78)$$

Since $\tau_n \leq \rho\tau_{n-1}$, it follows that $\theta_n \leq \psi\rho \leq 1 + \frac{1}{\psi}$. Additionally, we have

$$1 - \frac{\theta_{n-1}}{2\psi} \geq 1 - \frac{1}{2\psi} \left(\frac{1}{\psi} + \frac{1}{\psi^2} \right) \geq 1 - \frac{\psi+1}{2\psi^3} > 0, \quad \forall \psi \in [1, \phi].$$

Furthermore, noting that $\theta_n - \frac{\theta_n}{4} - \frac{\theta_n}{4} = \frac{\theta_n}{2} > \frac{\theta_n}{4}$, and combining this fact with (78), we conclude Lemma 5.6. \square

Theorem 5.7. *Under Assumptions 2.2, 2.3, and 5.5, suppose that $\{(z_n, x_n, y_n, \tau_n)\}$ is the sequence generated by Algorithm 3. Then, the sequence $\{(x_n, y_n)\}$ converges to a solution of (5).*

Proof. Let (x^*, y^*) be a saddle point of \mathcal{L} . Then we get, $2\tau_n\mathcal{G}(x_n, y_n) \geq 0, \forall n$. Now, (74) can be written as, $p_{n+1} \leq p_n - q_n, \forall n$, where

$$\begin{aligned} p_n &= \frac{\psi}{\psi-1} \|x^* - z_{n+1}\|^2 + \frac{1}{\beta} \|y^* - y_{n-1}\|^2 + \frac{\theta_{n-1}}{4} \|x_n - x_{n-1}\|^2, \\ q_n &= \theta_n \|x_n - z_{n+1}\|^2. \end{aligned} \quad (79)$$

Again, using Lemma 2.5, we obtain $\lim_{n \rightarrow \infty} p_n \in \mathbb{R}$ and $\lim_{n \rightarrow \infty} q_n = 0$. Moreover, from Proposition 5.4, we derive that $\lim_{n \rightarrow \infty} \|x_n - z_{n+1}\|^2 = 0$. Similarly, like in Theorem 3.6, combining with Proposition 5.4, we can show that $\lim_{n \rightarrow \infty} \|x_n - x_{n-1}\|^2 = 0$. Since $\lim_{n \rightarrow \infty} p_n \in \mathbb{R}$ and $\lim_{n \rightarrow \infty} q_n = 0$, both imply that $\{x_n\}, \{y_n\}$ and $\{z_n\}$ are bounded sequences. Let (\bar{x}, \bar{y}) be the subsequential limit of $\{(x_n, y_n)\}$. Then there exist a subsequence $\{(x_{n_k}, y_{n_k})\}$ of $\{(x_n, y_n)\}$ such that $\{(x_{n_k}, y_{n_k})\}$ converges to (\bar{x}, \bar{y}) , i.e., $\lim_{n \rightarrow \infty} x_{n_k} = \bar{x}$ and $\lim_{n \rightarrow \infty} y_{n_k} = \bar{y}$. Again, $\lim_{n \rightarrow \infty} \|x_n - z_{n+1}\|^2 = 0$ implies that $\lim_{n \rightarrow \infty} z_{n_k} = \bar{x}$. Furthermore, using Lemma 2.1 similarly like in Theorem 3.6, for all $(x, y) \in \mathbb{X} \times \mathbb{Y}$, we have

$$\begin{aligned} \langle x_{n_k} - z_{n_k} + \tau_{n_k-1}K^*y_{n_k-1} + \tau_{n_k-1}\nabla h(x_{n_k-1}), x - x_{n_k} \rangle &\geq \tau_{n_k-1}(f(x_{n_k}) - f(x)), \\ \langle (y_{n_k} - y_{n_k-1})/\beta + \tau_{n_k}Kx_{n_k}, y - y_{n_k-1} \rangle &\geq \tau_{n_k}(g^*(y_{n_k}) - g^*(y)). \end{aligned}$$

Recalling that both f, g^* are lower semi-continuous and letting $k \rightarrow \infty$, we derive

$$\langle K^*\bar{y} + \nabla h(\bar{x}), x - \bar{x} \rangle \geq f(\bar{x}) - f(x) \quad \text{and} \quad \langle K\bar{x}, y - \bar{y} \rangle \geq g^*(\bar{y}) - g^*(y). \quad (80)$$

Equation (80) implies that (\bar{x}, \bar{y}) is a saddle point of (5). Thus, all the above validation holds, including equation (79) replacing x^* by \bar{x} and y^* by \bar{y} . This implies that $\lim_{n \rightarrow \infty} p_{n_k} = 0$. Furthermore, the sequence $\{p_{n_k}\}$ is monotonically nonincreasing and bounded below. Thus, we have $\lim_{n \rightarrow \infty} p_n = 0$. Therefore, $\lim_{n \rightarrow \infty} z_n = \bar{x}$ and $\lim_{n \rightarrow \infty} y_n = \bar{y}$. Additionally, $\lim_{n \rightarrow \infty} \|x_n - z_{n+1}\|^2 = 0$ implies that $\lim_{n \rightarrow \infty} x_n = \bar{x}$. Hence, the proof is complete. \square

Theorem 5.8. (Sublinear rate of convergence) *Under Assumptions 2.2, 2.3, and 5.5, let $\{(z_n, x_n, y_n, \tau_n)\}$ be the sequence generated by Algorithm 3. Let (\bar{x}, \bar{y}) be a saddle point of \mathcal{L} . Then, there exists a constant $\eta_1 > 0$ such that*

$$\mathcal{G}(\tilde{x}_N, \tilde{y}_N) \leq \frac{1}{2\eta_1 N} \left(\frac{\psi}{\psi-1} \|x^* - z_2\|^2 + \frac{1}{\beta} \|y^* - y_0\|^2 + \frac{\theta_0}{4} \|x_1 - x_0\|^2 \right) \quad (81)$$

holds, where $N \geq 1$, and

$$\tilde{x}_N = \frac{1}{N} \sum_{n=1}^N x_n, \quad \tilde{y}_N = \frac{1}{N} \sum_{n=1}^N y_n.$$

Proof. Using the definition of q_n and p_n , we have

$$2\tau_n \mathcal{G}(x_n, y_n) \leq p_n - p_{n+1}, \quad \forall n$$

Again, from Proposition 5.4, we get $\tau_n \geq \eta_1 \forall n$, where $\eta_1 = \frac{\psi}{4(\bar{L}^2 + \beta\psi\|K\|^2)} \frac{1}{\tau_{\max}}$.

This implies that

$$2\eta_1 \mathcal{G}(x_n, y_n) \leq p_n - p_{n+1}. \quad (82)$$

Furthermore, summing over $n = 1, 2, \dots, N$, we obtain

$$\begin{aligned} 2\eta_1 \sum_{n=1}^N \mathcal{G}(x_n, w_n, y) &\leq p_1 - p_{N+1} \\ &\leq p_1 = \frac{\psi}{\psi-1} \|x^* - z_2\|^2 + \frac{1}{\beta} \|y^* - y_0\|^2 + \frac{\theta_0}{4} \|x_1 - x_0\|^2. \end{aligned} \quad (83)$$

Now, following similar calculations as in Theorem 4.1, we have

$$\begin{aligned} \mathcal{G}(\tilde{x}_N, \tilde{y}_N) &= \mathcal{L}(\tilde{x}_N, \bar{y}) - \mathcal{L}(\bar{x}, \tilde{y}_N) \\ &\leq \frac{1}{N} \sum_{n=1}^N \mathcal{L}(x_n, \bar{y}) - \mathcal{L}(\bar{x}, y_n) \\ &= \frac{1}{N} \sum_{n=1}^N \mathcal{G}(x_n, y_n) \leq \frac{p_1}{2\eta_1 N}. \end{aligned} \quad (84)$$

Thus, the proof is concluded. \square

6. Numerical Experiments

In this section, we provide numerical results on LASSO, Non-negative least squares, Elastic Net Regularization, and Fused LASSO for Algorithm 2 and Algorithm 3 and compare them with existing methods. Throughout this section, unless stated otherwise, we assume the following parameter values for aEGRPDA (Algorithm 3): $\psi = 1.5$, $\tau_0 = 10$, $\rho = \frac{1}{\psi} + \frac{1}{\psi^2}$, and $\tau_{\max} = 10^7$.

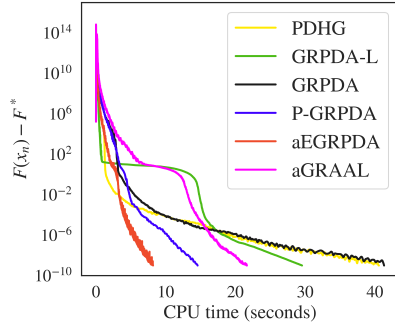
6.1. The LASSO Problem

The ℓ_1 -penalized linear regression or LASSO problem [34] is formulated as:

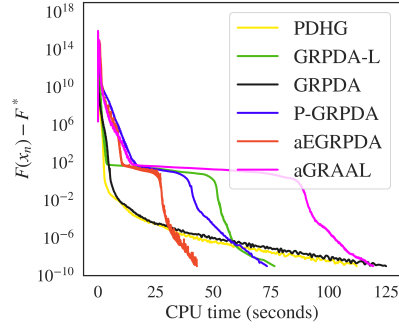
$$\min_{x \in \mathbb{R}^n} F(x) := \frac{1}{2} \|Kx - b\|^2 + \lambda \|x\|_1.$$

Here, rows of $K \in \mathbb{R}^{m \times n}$ represent predictor variables, λ is a regularization parameter, and $b \in \mathbb{R}^m$ is a given response vector. The objective is to find the unknown signal $x \in \mathbb{R}^n$. LASSO is a popular method in statistics for linear regression and is particularly interesting in compressive sensing when $n > m$, i.e., when the rank of K is less than n . Now, comparing LASSO with (1) gives $g(x) = \frac{1}{2}\|x - b\|^2$, $f(x) = \lambda\|x\|_1$, and $h = 0$. For our experiments, we set the *seed* to be 100. Next, following [8,9,24], we generate the required data for this problem as follows.

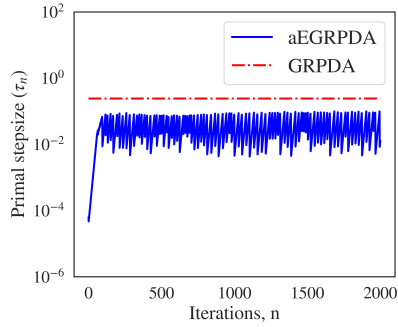
- (1) We generate $x^* \in \mathbb{R}^n$ as follows: the s nonzero coordinates of x^* are taken randomly using uniform normal distribution $\mathcal{N}(-10, 10)$ and the rest are put to 0. The entries of additional noise $\omega \in \mathbb{R}^m$ are drawn from $\mathcal{N}(0, 0.1)$ and we set $b = Kx^* + \omega$.
- (2) We generate the matrix K in one of the following ways:
 - (a) First, we generate a matrix B whose entries are drawn independently from $\mathcal{N}(0, 1)$. Then for $q \in (0, 1)$, we generate the matrix K by columns as follows: set $K_1 = \frac{B_1}{\sqrt{1-q^2}}$ and $K_j = qK_{j-1} + B_j$, where K_j, B_j are columns of K, B for $j = 2, 3, \dots, n$ respectively.
 - (b) All entries of K are sampled independently from $\mathcal{N}(0, 1)$.



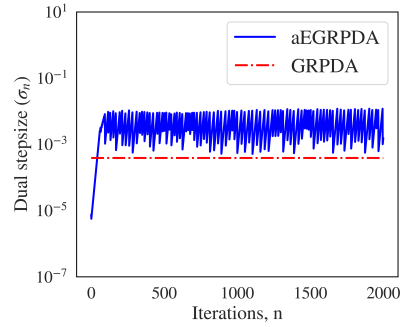
(a) $(m, n, q, s) = (500, 1000, 0.7, 10)$



(b) $(m, n, q, s) = (1000, 2000, 0.5, 100)$



(c) $(m, n) = (1000, 2000)$



(d) $(m, n) = (1000, 2000)$

Figure 2. Figures (a) and (b) compare the convergence plots of LASSO for different algorithms. Figures (c) and (d) illustrate the primal and dual stepsizes of aEGRPDA and GRPDA for LASSO.

We set the initial value for all algorithms as $x_0 = (0, \dots, 0)$, $y_0 = -b$, $\lambda = 0.1$ and iteration stops running when $F(x_n) - F^* < 10^{-9}$, where $F^* = \inf_x F(x)$ was computed by running our algorithm for sufficiently many iterations. We initialized the following

data for different algorithms:

- (1) PDHG [6]: $\tau = \frac{25}{\|K\|}, \sigma = \frac{0.04}{\|K\|}$, where $\|K\|^2 = \lambda_{\max}(K^*K)$.
- (2) GRPDA [8]: $\phi = 1.618, \tau = \frac{25}{\|K\|}, \sigma = \frac{0.04}{\|K\|}$, where $\|K\|^2 = \lambda_{\max}(K^*K)$.
- (3) GRPDA-L [10]: Set $\tau = \frac{1}{\|K\|}, \delta = 0.99, \mu = 0.7$, where δ and μ are involved in the inequality of the stopping criteria of GRPDA-L.
- (4) P-GRPDA (Algorithm 2): $\mu = 0.80, \psi = 1.618, \tau_0 = 10, \beta = 1/10$.
- (5) aGRPDA (Algorithm 3): $\beta = 0.1$.

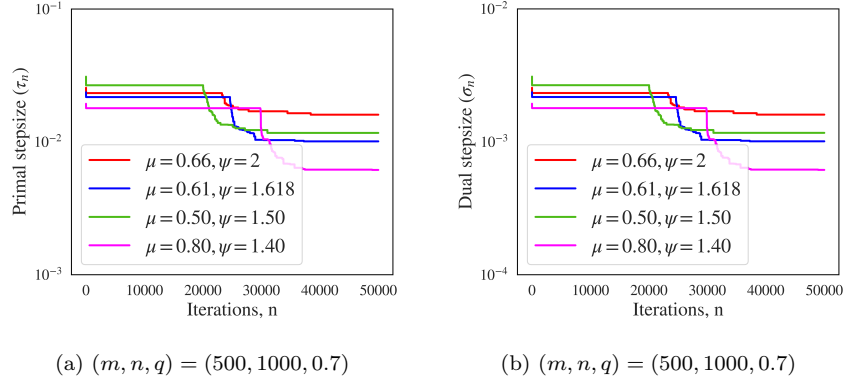


Figure 3. Primal and dual stepsizes of Lasso for P-GRPDA for different values of μ and ψ .

Figure 2 represents the decreasing behavior of $F(x_n) - F^*$ versus the CPU time in seconds, and Figure 3 shows the nonincreasing nature of the primal and dual stepsizes of the P-GRPDA algorithm. From Figure 2, we can see that both the oscillating primal and dual stepsizes of aGRPDA are bounded by the primal and dual stepsizes of GRPDA.

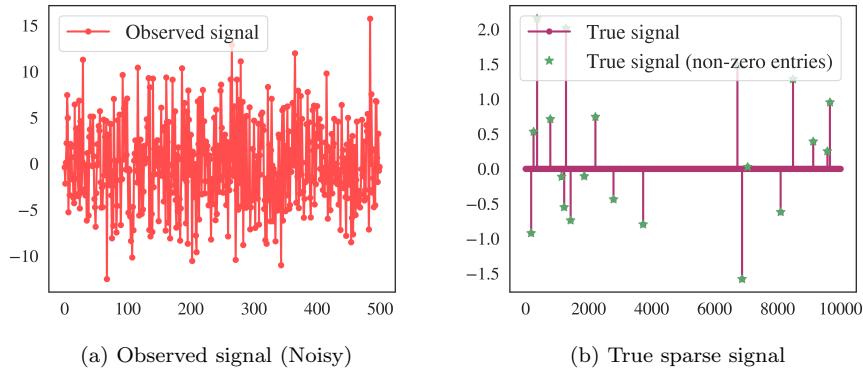


Figure 4. Comparison of recovered signals, observed signal, and convergence plots for P-GRPDA, GRPDA, and aGRPDA.

6.1.1. LASSO signal recovery

Next, we will perform the following numerical experiments on signal recovery for LASSO. Let $m = 500$ and $n = 10000$. Suppose that x^* is the true sparse signal,

and A is the random matrix whose elements are drawn from standard Gaussian distribution. Let $b = Ax^* + 0.1 * \nu$ be the observed signal with noise ν , where the elements of ν are drawn from $\mathcal{N}(0, 1)$. In this case, we set $\lambda = 0.05$. Our aim is to recover the nonzero elements of the true sparse signal x^* . Figure 5 collects the results of recovering the noisy signal using GRPDA, P-GRPDA, and aEGRPDA. It can be observed that all the spikes of the true sparse signals in Figure 4 are almost recovered by the above-mentioned algorithms. Figure 5 also illustrates the corresponding convergence behavior, where aEGRPDA demonstrates the most significant decrease of $F(x_n) - F^*$ followed by P-GRPDA and GRPDA.

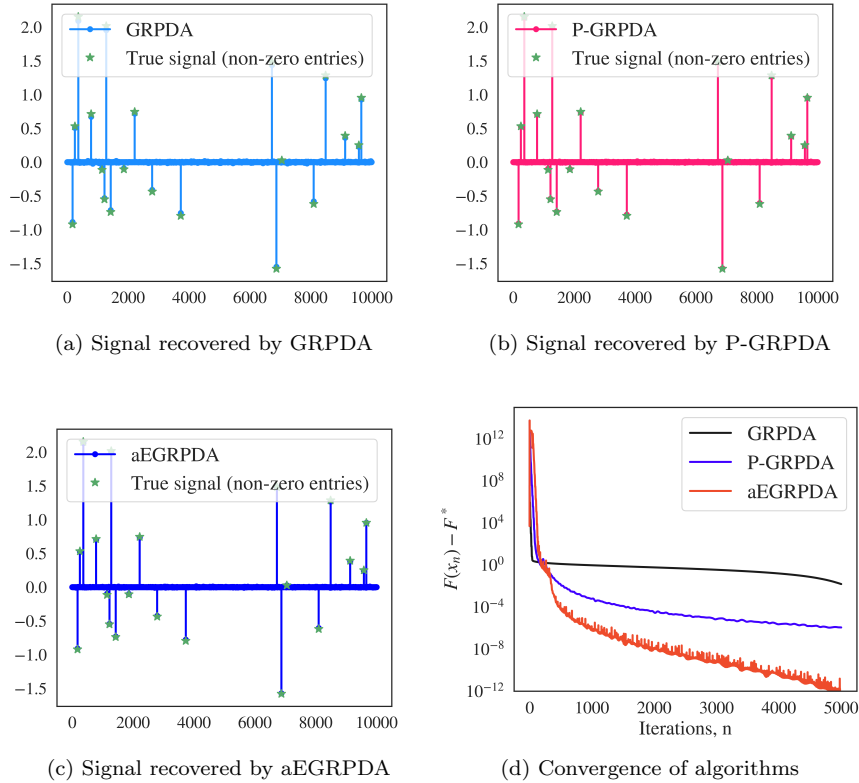


Figure 5. Comparison of recovered signals, observed signal, and convergence plots for P-GRPDA, GRPDA, and aEGRPDA.

6.2. Non-negative least squares

In this section, we consider another least square problem

$$\min_{x \in \mathbb{R}_+^n} F(x) := \frac{1}{2} \|Kx - b\|^2, \quad (85)$$

where $\mathbb{R}_+^n = \{x \in \mathbb{R}^n : x_i \geq 0, \forall 1 \leq i \leq n\}$, $K \in \mathbb{R}^{m \times n}$ and $b \in \mathbb{R}^m$. The objective (85) can also be expressed as

$$\min_{x \in \mathbb{R}^n} F(x) := \frac{1}{2} \|Kx - b\|^2 + i_{\mathbb{R}_+^n}(x). \quad (86)$$

Comparing (86) with (1) gives $h = 0, g = \frac{1}{2} \|\cdot - b\|^2$ and $f = i_{\mathbb{R}_+^n}(\cdot)$. The difference between LASSO and non-negative least squares is that the ℓ_1 regularization term is replaced by the *indicator function* $i_{\mathbb{R}_+^n}$. The proximal operator of f is nothing but the projection on the non-negative orthant \mathbb{R}_+^n . In this experiment, we consider random and real data as it was tested in [8]. For real data, we consider “i11c1850” and “i11c1033”, where $K \in \mathbb{R}^{m \times n}$ is the sparse matrix of sizes (1850, 712) and (1033, 320), respectively. The entries of b are drawn from the uniform normal distribution in (0, 1). For random data, we generate $K \in \mathbb{R}^{m \times n}$ randomly whose $\bar{d}mn$ elements are nonzero,

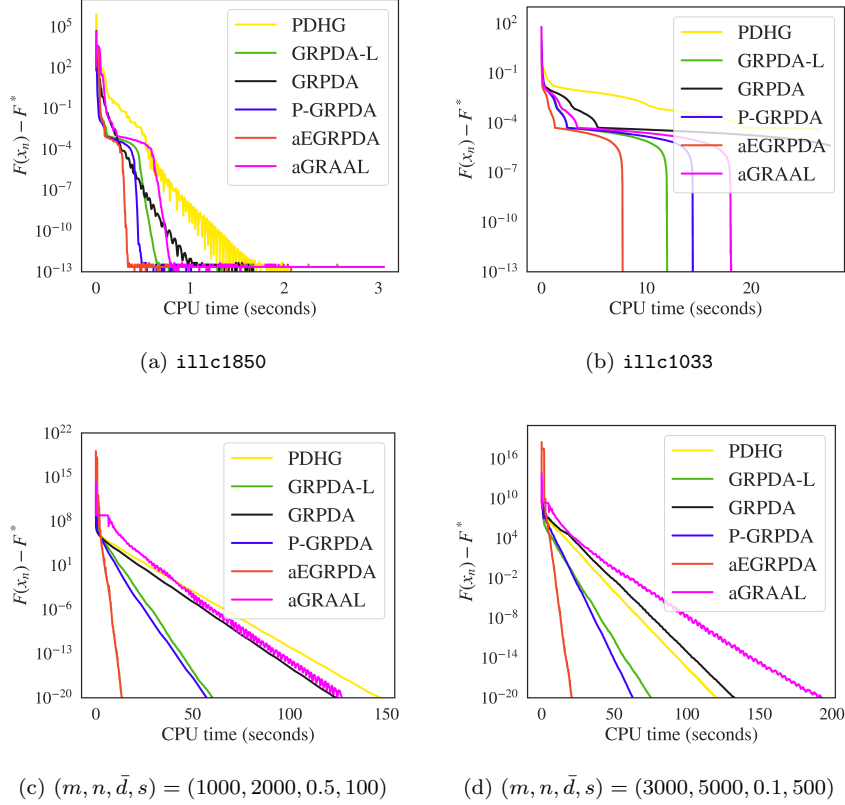


Figure 6. Real data: Comparison results of non-negative least squares for different algorithms for datasets i11c1850 and i11c1033. Random data: Comparison results of non-negative least squares for different algorithms.

where $0 < \bar{d} < 1$, see [8,24] for more details. In order to make $F^* = 0$, we set x^* to be a sparse vector whose s nonzero elements are drawn uniformly from $[0, 100]$. We also set $Kx^* = b$. For the datasets i11c1850 and i11c1033, all algorithms are terminated when $F(x_n) - F^* < 10^{-13}$ or after a maximum number of 20000 iterations. For random data, all algorithms are terminated when $F(x_n) - F^* < 10^{-20}$ or after a maximum number of 20000 iterations. From Figure 6, we observe that aEGRPDA gives better convergence bounds on each graph, followed by P-GRPDA, except for the dataset i11c1033.

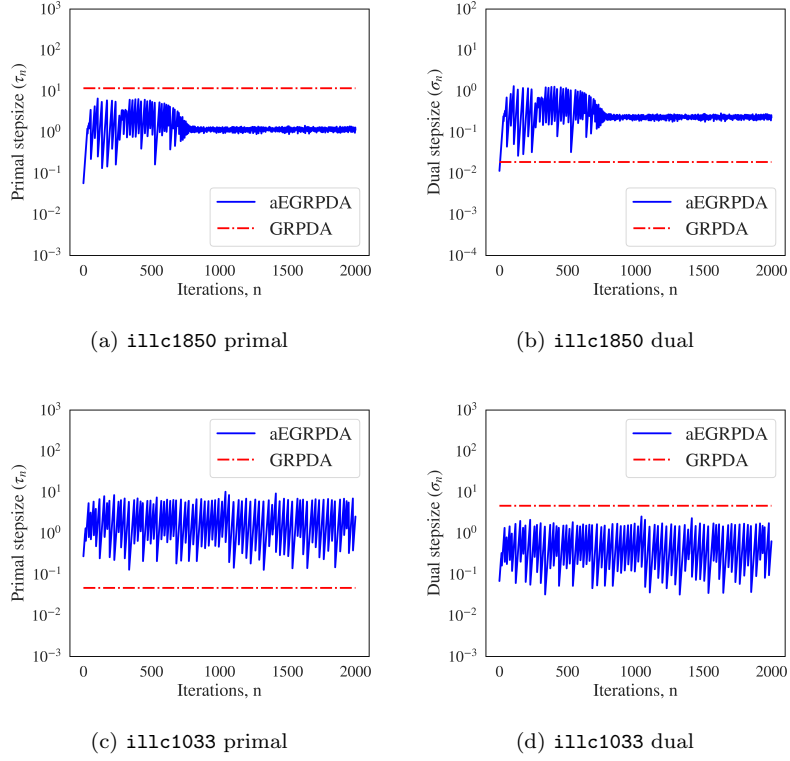


Figure 7. Primal-dual stepsizes of non-negative least squares for the dataset `illc1850` and `illc1033`.

6.3. Elastic Net regularization

The Elastic Net regularization problem [45] is written as

$$\min_{x \in \mathbb{R}^n} F(x) := \frac{1}{2} \|Kx - b\|^2 + \lambda_1 \|x\|_1 + \lambda_2 \|x\|^2, \quad (87)$$

where $K \in \mathbb{R}^{m \times n}$, $b \in \mathbb{R}^m$ and λ_1, λ_2 are regularization parameters. Comparing (87) with (1) gives $f(x) = \lambda_1 \|x\|_1$, $g(x) = \frac{1}{2} \|x - b\|^2$ and $h(x) = \lambda_2 \|x\|^2$. In this experiment,

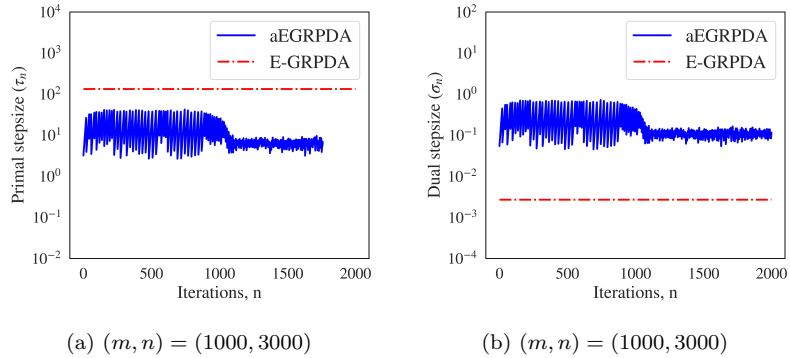


Figure 8. Primal and Dual stepsizes of Elastic Net for E-GRPDA and aEGRPDA.

the elements of K , i.e., $K_{i,j}$ for all i, j , are drawn using normal distribution in $(0, 0.01)$.

The entries of additional noise $\omega \in \mathbb{R}^m$ are drawn from $\mathcal{N}(0, 0.04)$ and we set $b = Kx^* + \omega$, where elements of x^* are generated from $\mathcal{N}(0, 1)$. In this experiment, we set $\lambda_1 = 0.01$ and $\lambda_2 = 0.003$. Since $h(x) = \lambda_2 \|x\|^2$, the Lipschitz constant \bar{L} of h is $2\lambda_2$. We set $x_0 = 0, y_0 = -b$ and other initial data are chosen as follows:

- (1) Condat-Vũ [13,38]: $\tau = \frac{4}{5\lambda_2}, \sigma = \frac{2\lambda_2}{3\|K\|^2}$, where $\|K\| = \sqrt{\lambda_{\max}(K^*K)}$.
- (2) EGRPDA [43]: $\tau = \frac{4}{5\lambda_2}, \sigma = \frac{2\lambda_2}{3\|K\|^2}, \psi = 1.618$.
- (3) P-GRPDA (Algorithm 2): $\psi = 1.93, \mu = 0.70, \mu' = 0.21, \beta = 0.12, \tau_0 = 10$.
- (4) aEGRPDA (Algorithm 3): $\beta = 0.25$.

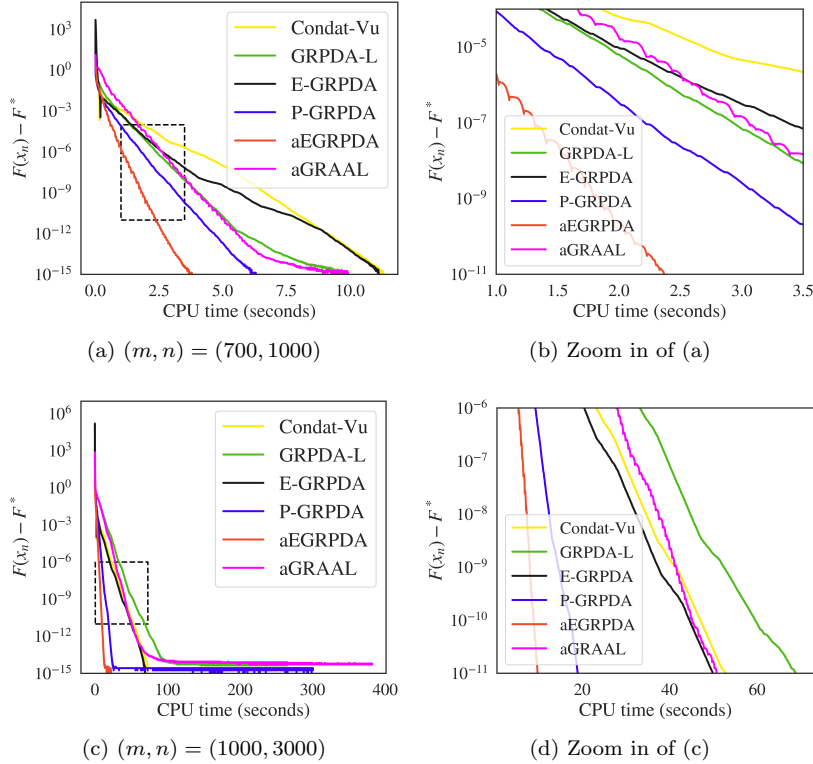


Figure 9. Comparison results of Elastic Net for different algorithms.

To apply GRPDA-L, we choose f as $f + h$, where its proximal operator corresponds to the weighted sum of the ℓ_1 -norm and ℓ_2 -norm, commonly referred to as the *soft-thresholding operator*. In this scenario, the parameters are set following [10]: $\beta = 1, \psi = 1.5$, and $\tau_0 = 10$, while the remaining initial parameters are consistent with those chosen for the LASSO problem. All algorithms are terminated when $F(x_n) - F^* < 10^{-15}$ or after a maximum of 30000 iterations. The numerical results are illustrated in Figure 8 and 9.

6.4. Fused Lasso

The Fused Lasso problem is written as

$$\min_{x \in \mathbb{R}^n} F(x) := \lambda_1 \|x\|_1 + \lambda_2 \|Dx\|_1 + \frac{1}{2} \|Ax - b\|^2. \quad (88)$$

Here, the difference matrix $D \in \mathbb{R}^{(n-1) \times n}$ is given by

$$K = D = \begin{bmatrix} -1 & 1 & 0 & \cdots & 0 \\ 0 & -1 & 1 & \cdots & 0 \\ \vdots & \vdots & \vdots & \ddots & \vdots \\ 0 & 0 & 0 & \cdots & -1 & 1 \end{bmatrix}.$$

In this experiment, the elements of $A = (A_{ij})$ and the elements of the additional noise vector $\omega \in \mathbb{R}^m$ are sampled from a normal distribution $\mathcal{N}(0, 0.01)$. The vector b is then constructed as $b = Kx^* + \omega$, where the entries of x^* are independently generated from $\mathcal{N}(0, 1)$. We set $\lambda_1 = 0.001$ and $\lambda_2 = 0.03$. For the data-fitting term $h(x) = \frac{1}{2} \|Ax - b\|^2$, its gradient is $\nabla h(x) = A^*(Ax - b)$. Therefore, the Lipschitz constant \bar{L} is $\|A^*A\|$, which corresponds to the largest eigenvalue of A^*A . We initialize the following data as follows:

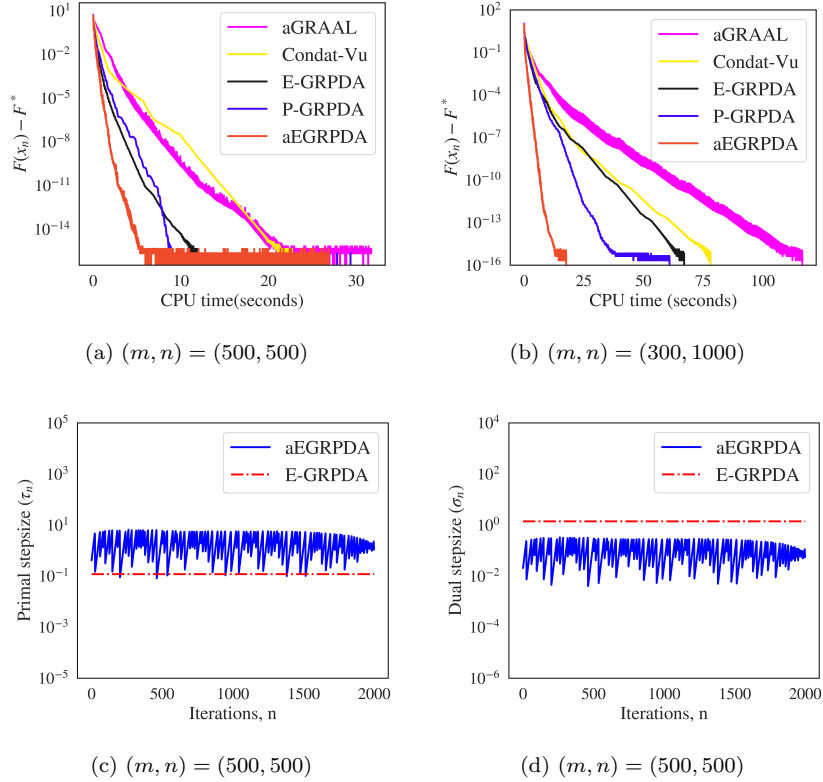


Figure 10. Figures (a) and (b) present the convergence plots for different algorithms of Fused Lasso. Figures (c) and (d) demonstrate the primal and dual stepsizes of Elastic Net for E-GRPDA and aEGRPDA.

- (1) Condat-Vũ: $\tau = 0.04 \cdot \frac{3}{5\|D\|}$, $\sigma = 25 \cdot \frac{10\|D\|}{9L^2}$, where $\|D\|$ is the square root of the largest eigenvalue of D^*D .
- (2) E-GRPDA: $\tau = 0.2 \cdot \frac{3}{5\|D\|}$, $\sigma = 5 \cdot \frac{10\|D\|}{9L^2}$, $\psi = 1.50$.
- (3) P-GRPDA (Algorithm 2): $\mu = 0.80$, $\mu' = 0.26$, $\psi = 1.618$, $\tau_0 = 10$, $\beta = 1/20$.
- (4) aEGRPDA (Algorithm 3): $\beta = 1/20$.

We terminate all algorithms when $F(x_n) - F^* < 10^{-16}$ or 10000 iterations reached.

Figure 10 presents the numerical graphs for this experiment.

7. Conclusion

In this work, we introduced two new stepsize rules for E-GRPDA (12), which do not need backtracking to remove the dependency on $\|K\|$ and \bar{L} . In the first stepsize rule, the primal stepsize τ_n converges, with its limit bounded below by a positive value. This crucial fact enabled us to establish both the global iterate convergence and the R-linear rate of convergence for Algorithm 2. Additionally, we extended the convergence region of the Algorithm 2 from $(1, \phi]$ to $(1, 1 + \sqrt{3})$ as it was done for GRPDA [9]. The second stepsize rule, motivated from [21,37], leverages the local stepsize inequality of E-GRPDA to establish the global convergence of Algorithm 3. Our proposed approaches were validated through experiments on a variety of convex optimization problems, including Lasso, Fused Lasso, Elastic Net, and Non-negative Lasso. We illustrated the decreasing behavior of $F(x_n) - F^*$ with CPU time (in seconds) of our algorithms in comparison to existing methods. We also conducted signal recovery experiments for Lasso, highlighting the advantages of our approaches. Future direction includes investigating the acceleration of the Algorithm 2 to achieve an $\mathcal{O}(1/N^2)$ convergence rate, akin to GRPDA and E-GRPDA [8,10,43]. Additionally, it would be interesting to explore Algorithm 2 to the settings when h is locally smooth.

Acknowledgements

We thank Dr. Felipe Atenas for the valuable feedback on this paper. The research of Santanu Soe was supported by the Prime Minister’s Research Fellowship program (Project number SB23242132MAPMRF005015), SERB, India, and the Melbourne Research Scholarship. Matthew K. Tam was supported in part by Australian Research Council grant DP230101749. V. Vetrivel was supported by the Department of Science and Technology, SERB, India, under the project ‘FIST Program-2022’ (SR/FST/MSIAI/2022/107).

Data availability

The real datasets, `illc1033` and `illc1850`, used in the Non-negative Lasso experiment, are available at [5]. Additional datasets generated during the numerical experiments are referenced in [8,24]. The source code for this paper is available from the corresponding author upon reasonable request.

Conflict of interest

The authors declare that they have no conflict of interest in this paper.

References

- [1] B. Abbas and H. Attouch. Dynamical systems and forward-backward algorithms associated with the sum of a convex subdifferential and a monotone cocoercive operator.

- Optimization*, 64(10):2223–2252, 2015.
- [2] H. H. Bauschke and P. L. Combettes. *Convex analysis and monotone operator theory in Hilbert spaces*. Springer, New York, 2011.
 - [3] A. Beck. *First-order methods in optimization*. SIAM, Philadelphia, 2017.
 - [4] D. P. Bertsekas and E. M. Gafni. *Projection methods for variational inequalities with application to the traffic assignment problem*, pages 139–159. Springer, Berlin, 1982.
 - [5] R. F. Boisvert, R. Pozo, K. Remington, R. F. Barrett, and J. J. Dongarra. Matrix market: a web resource for test matrix collections. *Quality of Numerical Software: Assessment and Enhancement*, pages 125–137, 1997.
 - [6] A. Chambolle and T. Pock. A first-order primal-dual algorithm for convex problems with applications to imaging. *Journal of Mathematical Imaging and Vision*, 40:120–145, 2011.
 - [7] A. Chambolle and T. Pock. On the ergodic convergence rates of a first-order primal–dual algorithm. *Mathematical Programming*, 159(1):253–287, 2016.
 - [8] X. Chang and J. Yang. A golden ratio primal–dual algorithm for structured convex optimization. *Journal of Scientific Computing*, 87:1–26, 2021.
 - [9] X. Chang and J. Yang. GRPDA revisited: Relaxed condition and connection to Chambolle-Pock’s primal-dual algorithm. *Journal of Scientific Computing*, 93(3):70, 2022.
 - [10] X.-K. Chang, J. Yang, and H. Zhang. Golden ratio primal-dual algorithm with linesearch. *SIAM Journal on Optimization*, 32(3):1584–1613, 2022.
 - [11] P. Chen, J. Huang, and X. Zhang. A primal-dual fixed point algorithm for minimization of the sum of three convex separable functions. *Fixed Point Theory and Applications*, 2016:1–18, 2016.
 - [12] P. L. Combettes and V. R. Wajs. Signal recovery by proximal forward-backward splitting. *Multiscale Modeling & Simulation*, 4(4):1168–1200, 2005.
 - [13] L. Condat. A primal–dual splitting method for convex optimization involving Lipschitzian, proximable and linear composite terms. *Journal of Optimization Theory and Applications*, 158(2):460–479, 2013.
 - [14] D. Gabay and B. Mercier. A dual algorithm for the solution of nonlinear variational problems via finite element approximation. *Computers & Mathematics with Applications*, 2(1):17–40, 1976.
 - [15] R. Glowinski and A. Marroco. Sur l’approximation, par éléments finis d’ordre un, et la résolution, par pénalisation-dualité d’une classe de problèmes de dirichlet non linéaires. *Revue Française D’automatique, Informatique, Recherche Opérationnelle. Analyse Numérique*, 9(R2):41–76, 1975.
 - [16] T. Goldstein, M. Li, and X. Yuan. Adaptive primal-dual splitting methods for statistical learning and image processing. *Advances in Neural Information Processing Systems*, 28, 2015.
 - [17] B. He, S. Xu, and X. Yuan. On convergence of the Arrow–Hurwicz method for saddle point problems. *Journal of Mathematical Imaging and Vision*, 64(6):662–671, 2022.
 - [18] B. He and X. Yuan. Convergence analysis of primal-dual algorithms for a saddle-point problem: from contraction perspective. *SIAM Journal on Imaging Sciences*, 5(1):119–149, 2012.
 - [19] P. Latafat, A. Themelis, L. Stella, and P. Patrinos. Adaptive proximal algorithms for convex optimization under local Lipschitz continuity of the gradient. *arXiv preprint arXiv:2301.04431v4*, 2023.
 - [20] P.-L. Lions and B. Mercier. Splitting algorithms for the sum of two nonlinear operators. *SIAM Journal on Numerical Analysis*, 16(6):964–979, 1979.
 - [21] Y. Malitsky. Golden ratio algorithms for variational inequalities. *Mathematical Programming*, 184(1-2):383–410, 2020.
 - [22] Y. Malitsky and K. Mishchenko. Adaptive gradient descent without descent. In *International Conference on Machine Learning*, pages 6702–6712. PMLR, 2020.
 - [23] Y. Malitsky and K. Mishchenko. Adaptive proximal gradient method for convex optimization. *arXiv preprint arXiv:2308.02261v2*, 2023.
 - [24] Y. Malitsky and T. Pock. A first-order primal-dual algorithm with linesearch. *SIAM*

- Journal on Optimization*, 28(1):411–432, 2018.
- [25] Y. Malitsky and M. K. Tam. A first-order algorithm for decentralised min-max problems. *arXiv preprint arXiv:2308.11876*, 2023.
- [26] A. Nedić and A. Ozdaglar. Subgradient methods for saddle-point problems. *Journal of Optimization Theory and Applications*, 142:205–228, 2009.
- [27] Y. Nesterov. Gradient methods for minimizing composite functions. *Mathematical Programming*, 140(1):125–161, 2013.
- [28] N. Parikh and S. Boyd. Proximal algorithms. *Foundations and Trends in Optimization*, 1(3):127–239, Jan. 2014.
- [29] T. Pock and A. Chambolle. Diagonal preconditioning for first order primal-dual algorithms in convex optimization. In *2011 International Conference on Computer Vision*, pages 1762–1769. IEEE, 2011.
- [30] E. K. Ryu and W. Yin. *Large-scale convex optimization: algorithms & analyses via monotone operators*. Cambridge University Press, 2022.
- [31] A. Salim, L. Condat, K. Mishchenko, and P. Richtárik. Dualize, split, randomize: Toward fast nonsmooth optimization algorithms. *Journal of Optimization Theory and Applications*, 195(1):102–130, 2022.
- [32] E. Y. Sidky, J. H. Jørgensen, and X. Pan. Convex optimization problem prototyping for image reconstruction in computed tomography with the Chambolle–Pock algorithm. *Physics in Medicine & Biology*, 57(10):3065, 2012.
- [33] M. K. Tam and D. J. Uteda. Bregman golden ratio algorithms for variational inequalities. *Journal of Optimization Theory and Applications*, 199(3):993–1021, 2023.
- [34] R. Tibshirani. Regression shrinkage and selection via the Lasso. *Journal of the Royal Statistical Society Series B: Statistical Methodology*, 58(1):267–288, 1996.
- [35] R. Tibshirani, M. Saunders, S. Rosset, J. Zhu, and K. Knight. Sparsity and smoothness via the fused Lasso. *Journal of the Royal Statistical Society Series B: Statistical Methodology*, 67(1):91–108, 2005.
- [36] H. Uzawa. Iterative methods for concave programming. *Studies in Linear and Nonlinear Programming*, 6:154–165, 1958.
- [37] M.-L. Vladarean, Y. Malitsky, and V. Cevher. A first-order primal-dual method with adaptivity to local smoothness. *Advances in Neural Information Processing Systems*, 34:6171–6182, 2021.
- [38] B. C. Vũ. A splitting algorithm for dual monotone inclusions involving cocoercive operators. *Advances in Computational Mathematics*, 38(3):667–681, 2013.
- [39] M. Yan. A new primal–dual algorithm for minimizing the sum of three functions with a linear operator. *Journal of Scientific Computing*, 76:1698–1717, 2018.
- [40] J. Yang and Y. Zhang. Alternating direction algorithms for ℓ_1 -problems in compressive sensing. *SIAM Journal on Scientific Computing*, 33(1):250–278, 2011.
- [41] M. Yuan and Y. Lin. Model selection and estimation in regression with grouped variables. *Journal of the Royal Statistical Society Series B: Statistical Methodology*, 68(1):49–67, 2006.
- [42] X. Zhang, M. Burger, and S. Osher. A unified primal-dual algorithm framework based on Bregman iteration. *Journal of Scientific Computing*, 46:20–46, 2011.
- [43] D. Zhou, X. Chang, J. Yang, et al. A new primal-dual algorithm for structured convex optimization involving a Lipschitzian term. *Pacific Journal of Optimization.*, 18(2):497–517, 2022.
- [44] M. Zhu and T. Chan. An efficient primal-dual hybrid gradient algorithm for total variation image restoration. *UCLA Cam Report*, 34:8–34, 2008.
- [45] H. Zou and T. Hastie. Regularization and variable selection via the elastic net. *Journal of the Royal Statistical Society Series B: Statistical Methodology*, 67(2):301–320, 2005.